Oxidative stress-mediated inhibition of intestinal epithelial cell proliferation by silver nanoparticles

Christie McCracken,[†] Andrew Zane,[‡] Deborah A. Knight,[†] Prabir K. Dutta,[§] and W. James Waldman[†]

[†]Department of Pathology, The Ohio State University College of Medicine, Columbus, Ohio 43210, United States

[‡]The Henry M. Jackson Foundation for the Advancement of Military Medicine, San Antonio, Texas 78234, United States

[§]Department of Chemistry and Biochemistry, The Ohio State University, Columbus, Ohio 43210, United States

Abstract:

Use of silver nanoparticles (NP) is of interest in the food and food packaging industries for their antimicrobial properties. In order to investigate potential consequences of Ag NP ingestion, this study was performed in the intestinal epithelial cell line C2BBe1. Ag NP were synthesized and characterized prior to biological experiments. The Ag NP had an average diameter of 23 nm as determined by TEM analysis. Treatment of proliferating cells (< 10,000 cells/cm^2) with low doses of Ag NP (0.25 µg/cm^2 or 1.25 µg/mL) for 24 hours induced 20% necrotic cell death and an 80% reduction in metabolic activity. Ag NP treatment of proliferating cells for 24 hours at 0.25 µg/cm^2 induced oxidative stress in cells as indicated by a decrease in the GSH/GSSG ratio. Ag NP treatment with 0.25 µg/cm^2 also induced G2/M phase cell cycle arrest and a complete inhibition of Ag NP. An *in vitro* digestion treatment of Ag NP prior to cell exposure required slightly higher doses (0.5 µg/cm^2 or 2.5 µg/mL) to induce the same toxicity, likely due to increased species adsorbed to the surface causing slower Ag dissolution. Treatment of cells with silica, titania, and ZnO NP induced at least partial inhibition of cell proliferation at doses of 10 µg/cm^2 (50 µg/mL), but the Ag NP-induced inhibition of cell proliferation at doses 40 times lower reveals a unique mechanism of Ag NP in these cells. Our results in proliferating cells suggest that Ag NP-induced oxidative stress leads to cell cycle arrest and the inhibition of cell proliferation. However, toxicity and induction of oxidative stress was not observed in confluent C2BBe1 cells (>100,000 cells/cm^2) treated with up to 10 µg/cm^2 (50 µg/mL) Ag NP, suggesting that these cells are not as sensitive to Ag NP. This is likely due to exposure of each cell to a smaller number of Ag NP when the cells are confluent in addition to decreased metabolic activity and increased resistance to toxic agents in confluent cells. Based on these studies, Ag NP ingestion may be able to slow proliferation of

stem cells of the intestinal crypt and this is something that needs to be investigated further. The largest effects may be seen in diseased intestines where the epithelium is compromised.

Introduction:

Nanotechnology is being increasingly used in a variety of industries for the unique properties materials display at the nanoscale due to a larger surface area per unit mass and thus an increase in the number of surface atoms available to react. Silver nanoparticles (Ag NP) are commonly being used for their increased catalytic activity.[1] The optical properties of Ag NP allow them to be used as chemical and biological sensors.[1] Another major use of Ag NP is for stronger antimicrobial activity.[1] Silver has been used for centuries for its antimicrobial properties in water purification, in wound dressings to promote healing, for prevention and treatment of infection, and other medical applications,[2] and the largest use of Ag NP today is still for its antimicrobial effects. The Project on Emerging Nanotechnologies, which attempts to inventory consumer products containing nanotechnologies, currently lists 438 products containing silver nanoparticles.[3] These include textiles such as sheets, towels, and socks, curling irons, air purifiers, a stuffed animal, and toothbrushes, all utilizing the antimicrobial properties of Ag NP. The food and food packaging industries are also interested in utilizing Ag for its antibacterial properties and 41 of the products listed by the Project on Emerging Nanotechnologies are in the Food and Beverage category.[3] These include Ag supplements, cookware, utensils, and appliances coated with Ag NP, and Ag NP incorporated into food storage containers to prevent food spoilage. In addition to direct consumption of Ag NP used in foods, some fraction of Ag NP incorporated into food packaging and food contact materials may be transferred to food, further increasing Ag NP consumption.

It has been shown that Ag NP can mediate their antimicrobial effects through oxidative stress, which can then damage bacterial membranes. Electron spin resonance has been used to detect radicals on the surface of 13.5 nm Ag NP.[4] While this microbial toxicity has great potential utility, the same mechanism may contribute to cytotoxicity to mammalian cells. In medical

applications, care can be made to use doses of Ag NP that will be toxic to microbes but not human cells. However, the dose of Ag NP is less controllable when these nanoparticles are being ingested due to use in food and food contact materials.

Ingested Ag NP will be transported through the digestive tract, exposed to digestive enzymes, and excreted from the body if not absorbed in the intestines, as occurs with most non-nutrient components of our food. Intestinal epithelial cells within the intestines are responsible for transport of nutrients from the intestinal lumen to the bloodstream to be used by the rest of the body. Nanoparticles are likely to come into the most contact with these cells after ingestion due to Ag NP release from the food matrix due to digestion and the longer transit time of food through the intestines compared to the mouth and stomach. In order to gain access to the circulation to be more widely distributed throughout the body, Ag NP will have to first be transported across the intestinal epithelium. *In vivo* studies with PLGA, polystyrene, and thiol-organosilica nanoparticles between 50-100 nm have shown that nanoparticles are internalized by and transported across the intestinal epithelium into the circulation more readily than larger particles between 100-10,000 nm.[5-7] Studies where 10-60 nm Ag NP were orally administered to rodents have also shown incorporation of Ag NP into intestinal epithelial cells and transport of nanoparticles across the epithelium.[8-10] Thus, interaction of Ag NP with intestinal epithelial cells will be important for the systemic effects of Ag NP ingestion, and intestinal epithelial cells serve as a relevant *in vitro* model to study impact of nanoparticle ingestion.

As the use of Ag NP has increased, there has been concern about environmental accumulation of Ag NP and the potential health impacts of Ag NP in humans. This has led to studies in various systems exploring Ag NP cytotoxicity and the mechanism of response to Ag NP in several cell models. These studies have described an oxidative stress-mediated mechanism of

cytotoxicity in cells which leads to DNA damage, mitochondrial damage, cell cycle arrest, and apoptosis.[11-13] Studies in intestinal epithelial cell models have reported Ag NP toxicity including decreased cell viability, formation of reactive oxygen species (ROS), decreased mitochondrial function, increased IL-8 generation by cells, and DNA damage.[14-17] However, there has been less thorough investigation of the mechanism of Ag NP toxicity in intestinal epithelial models and no investigation of Ag NP effects on cell proliferation. It is known that oxidative stress plays a role in inflammation and disease progression in the intestines, so an increase in oxidative stress by Ag NP in the intestines may be particularly problematic for those with intestinal pathologies.[18]

In this study, we utilize the intestinal epithelial C2BBe1 model to investigate the mechanism of 23 nm Ag NP cytotoxicity on proliferating and confluent cells. Low dose Ag NP treatment at 0.25 μg/cm^2 (1.25 μg/mL) induced 20% necrosis and an 80% loss of metabolic activity in proliferating cells (defined as < 10,000 cell/cm^2). Ag NP treatment in proliferating cells decreased the ratio of reduced to oxidized glutathione in cells, indicating induction of oxidative stress. Ag NP treatment at 0.25 μg/cm^2 also completely inhibited cell proliferation and induced G2/M phase cell cycle arrest. Ag NP that underwent simulated *in vitro* digestion before cell exposure required a slightly higher dose (0.5 μg/cm^2) to induce the same inhibition of cell proliferation, likely due to slower dissolution of Ag ions because of greater protein adsorption to the NP surface. Inhibition of cell proliferation at low doses (0.25 μg/cm^2) was unique to Ag and not observed after SiO_2, TiO_2, or ZnO NP treatment, although ZnO inhibited cell proliferation at higher doses (10 μg/cm^2). Based on this, we are hypothesizing that Ag NP are increasing cellular oxidative stress, leading to DNA damage and cell cycle arrest, and thus inhibiting cell cycle proliferation. Ag NP were not directly toxic to confluent cells (defined as 100,000 cells/cm^2) up to doses of 10 μg/cm^2.

Materials and Methods:

All Ag nanoparticle synthesis and characterization (dynamic light scattering and zeta potential measurements, TEM analysis, infrared spectroscopy, Raman spectroscopy, X-ray diffraction, and atomic absorption spectroscopy) and simulated gastrointestinal digestion of nanoparticles was performed by Andrew Zane in Dr. Prabir Dutta's laboratory in The Ohio State University Department of Chemistry and Biochemistry.

Nanoparticle synthesis

Silver nanoparticles (~20 nm) were prepared as follows. A 200 mL solution of 0.25 mM $AgNO_3$ and 0.25 mM trisodium citrate is prepared in purified water and stirred for 30 minutes. Six mL of a 10 mM NaBH4 solution is slowly added under stirring. The solution is stirred for 30 minutes, then left at room temperature for 24 hours. Particles are washed twice by centrifugation at 290,000×*g* for 30 minutes, removal of supernatant, and redispersion in purified water.

Simulated gastrointestinal digestion of Ag

As described in an earlier publication, pepsin, pancreatin, and bile salts were used to simulate the gastric and small intestinal digestive environments *in vitro*.[19] The concentrations used were based on *in vitro* digestion methods used in previously published studies.[20-23] Briefly, pepsin (stomach, 146 U/ml, Sigma-Aldrich), pancreatin (intestinal enzyme mixture, 2 mg/ml, Sigma-Aldrich), and bile extract (porcine, 0.024 mg/ml, Sigma-Aldrich) were dissolved in water and adjusted to a pH of 2 (pepsin) or 7 (pancreatin and bile extract).

To simulate the digestive process, silver nanoparticles (50 mg/L) were incubated sequentially in the pepsin, pancreatin, and bile extract solutions for one hour each at 37ºC. Subsequent to each incubation, the nanoparticles were pelleted by centrifugation (200,000×*g* for

30 minutes) and resuspended in the next solution. After incubation in the bile extract, nanoparticles were centrifuged, resuspended in phosphate-buffered saline (PBS) and used for biological studies.

Particle Size and Surface Charge

A Zetasizer Nano ZS (Malvern, Westborough, MA) was used to measure the zeta potential of the as-prepared and digested silver nanoparticles. The Nano ZS uses a 633 nm laser as its light source. For zeta potential measurements, a forward angle of 12° was used for collecting light. The default Smoluchowski model in the software program was used. Each measurement included 20 runs, and monomodal analysis provided by the vendor was used for analysis. Samples were titrated versus pH using an attached MPT-2 Autotitrator. The titrator was supplied with 0.1 M HCl and 1.0 M HCl. Three replicate measurements were taken at each pH with a two minute pause between all measurements.

TEM Images of As-Synthesized Silver Nanoparticles

Images were taken using a Tecnai F20 Transmission Electron Microscope. Ten mg/L solution of as-prepared silver nanoparticles in ethanol was prepared and sonicated for 30 minutes. The solution was dropped on to lacey carbon copper TEM grids (Ted Pella, Inc., Redding, CA) and allowed to dry for several hours.

Infrared Spectroscopy

Diffuse reflectance infrared Fourier transform spectroscopy (DRIFTS) was performed on as-prepared silver nanoparticles and digested silver nanoparticles. For the digested silver, after the final digestion step, the particles were washed twice with water. The digested particles were isolated by centrifugation and frozen with liquid nitrogen, then placed in a Millrock Bench Top Manifold Freeze Dryer (Millrock, Inc. Kingston, NY) to preserve any potential coating. The as-synthesized silver nanoparticles were washed twice, redispersed in water, frozen with liquid

nitrogen, and placed in the freeze dryer. DRIFTS analysis was performed with a Spectrum 400 FTIR Imaging System (Perkin Elmer, Waltham, MA). Scans were performed in percent reflectance mode, a KBr background was collected, and then the samples were added to the cell (approximately 10% wt. in KBr), and the spectrum recorded. Kubelka Munk analysis was performed with instrument software.

Raman Spectroscopy

Raman spectroscopy was recorded with a Renishaw InVia Raman Microscope using a 633 nm laser source and a CCD detector. For the digested silver, after the final digestion step, the particles were washed twice with water. The digested particles were isolated by centrifugation and frozen with liquid nitrogen, then placed in a Millrock Bench Top Manifold Freeze Dryer (Millrock, Inc. Kingston, NY) to preserve any potential coating. The as-synthesized silver nanoparticles were washed twice, redispersed in water, frozen with liquid nitrogen, and placed in the freeze dryer.

Atomic Absorption Spectroscopy

Atomic absorption spectroscopy was performed to test for the presence of dissolved silver ions after incubation of both as-prepared Ag and digested Ag nanoparticles in DMEM cell culture media for 0, 1, and 2 days. A Buck Scientific Accusys 211 spectrophotometer (East Norwalk, CT) was used with a Ag hollow cathode lamp (Heraeus). Standard solutions were diluted from 1000 ppm standard prepared by dissolving $AgNO_3$.

X-ray Photoelectron Spectroscopy

X-ray photoelectron spectroscopy (XPS) surface analysis of as-prepared and digested silver nanoparticles was carried out using a Kratos Axis Ultra system (Kratos Analytical, Manchester, UK) equipped with monochromated Al radiation (1486.6 eV). All binding energies for different elements were calibrated with respect to the C 1s line at 285 eV.

Cell culture

C2BBe1 cells were obtained from the American Type Culture Collection (Manassas, VA) at passage 47 (as specified by the vendor). The majority of these experiments were performed with cells between passages 75-84. Cells were cultured in Dulbecco's Modified Eagle Medium (DMEM; Life Technologies, Grand Island, NY) supplemented with 10% fetal bovine serum (FBS; Serum Source International, Inc., Charlotte, NC), 1 mM sodium pyruvate, 2 mM L-glutamine, 0.3% penicillin/streptomycin, 0.3 ug/mL Amphotericin B (fungizone), and 10 µg/mL transferrin (all from Life Technologies). Cells were incubated in 5% CO_2/95% room air at 37°C. Cells were passaged every 5-7 days and plated on flasks or plates pre-coated with collagen I (0.05 mg/mL, rat tail, Life Technologies). Cells were incubated at least 24 hours prior to treatment with nanoparticles.

Treatment of cells with nanoparticles

Non-silver nanoparticles were weighed and sterilized by steam-sterilization, then suspended in PBS to make a 1 mg/mL solution to use to treat cells. After silver synthesis, nanoparticles were collected by ultracentrifugation and resuspended in water, generally to a concentration of 0.1 mg/mL. Immediately prior to treating cells, nanoparticle solutions were sonicated using a VC130 Sonics Vibra-Cell sonicator (Sonic Materials, Inc. Norwalk, CT) pulsing for one second on, one second off for approximately 15 seconds in order to break up nanoparticle agglomerates before exposing them to cells. Nanoparticles were added to cells at the appropriate dose (between 0.05 and 10 µg/cm^2). To ensure consistency, doses were based on the area of the cell culture well (available from Corning for each plate sized used) rather than volume added to cells. To promote contact of nanoparticles with cells, plates were centrifuged at 300×*g* for 15 minutes.

TEM of nanoparticle-treated cells

To verify that treated cells internalized nanoparticles, TEM was performed. Cells were grown to near confluence in a 6-well tissue culture plate. Cells were then treated with nanoparticles and briefly centrifuged. After a 24-hour incubation at 37°C, the treated cells were washed twice with PBS before detachment with trypsin. Detached cells were washed with PBS and resuspended in 3% glutaraldehyde in PBS. Incubation steps were carried out at room temperature on a Lab Line orbital shaker (Barnstead/Thermolyne, Melrose Park, IL) operating at 700 rpm. The cell suspension was centrifuged at 1000×g for 5 minutes between each processing step. Fixed cells were washed twice with sodium cacodylate buffer (pH 7.4, 10 minutes each), then post-fixed in 1% osmium tetroxide in sym-collidine buffer (pH 7.6) for 1 hour at room temperature. Following two washes with s-collidine buffer (10 minutes each) the Ag-treated cells were en-bloc stained with a saturated aqueous uranyl acetate solution (pH 3.3) for 1 hour. Digested Ag-treated cells were not stained with the uranyl acetate to decrease contrast. All cells were dehydrated in a graded ethanol series up to absolute (10 minutes each). Acetone was used as the transitional solvent for two 10-minute washes. Cells were infiltrated overnight with a 1:1 mixture of acetone and Spurr's epoxy resin (Electron Microscopy Sciences, Fort Washington, PA). Finally, the cells were centrifuged and the pellet was placed into BEEM™ embedding capsules containing 100% Spurr's resin. Polymerization of epoxy blocks was carried out at 70° C overnight. Polymerized blocks were sectioned with a Leica Ultracut UCT ultramicrotome (Leica Microsystem GmbH, Wein, Austria). Ultrathin (80 nm) sections were collected on 200 mesh copper grids (Electron Microscopy Sciences) and post-stained with lead citrate (3 minutes). Electron micrographs were generated on with a JEOL JEM-1400 TEM (JEOL Ltd. Tokyo, Japan) equipped with a Veleta digital camera (Olympus Soft Imaging Solutions GmbH, Münster, Germany).

Toxicity assays

For the 24-hour acute toxicity assays described below (Sytox Red, Annexin V, LDH, and MTT), cells were seeded in 24-well tissue culture plates at a density of 2×10^4-1×10^5 cells/well and grown to 90-100% confluency. For the Sytox Red and Annexin V assays performed with proliferating cells, cells were plated in 6-well tissue culture plates at a density of 5×10^4-1×10^5 cells/well the day before treatment with Ag nanoparticles. The LDH and MTT assays in proliferating cells were performed on cells seeded in 24-well tissue culture plates at a density of 1×10^4 cells/well the day before treatment with Ag NP.

Sytox Red staining

To evaluate necrotic cell death (cellular membrane damage) in nanoparticle-treated cells, cells were stained with Sytox Red Dead Cell Stain (Life Technologies) and analyzed by flow cytometry. Cells were treated with nanoparticles for 24 hours, then detached from the culture plate with trypsin, suspended in 1 mL calcium- and magnesium-free Hanks Balanced Salt Solution (HBSS, Life Technologies), and stained with 1 µL of the Sytox Red Dead Cell Stain. Samples were incubated for at least 15 minutes at room temperature before analyzing for fluorescence using a FACScalibur flow cytometer (BD Biosciences) at an excitation wavelength of 635 nm. All experimental conditions were performed in triplicate. As a positive control for cell death, a subset of wells were treated with 20 mM hydrogen peroxide (H_2O_2) in DMEM at the same time as nanoparticle treatment, 24 hours prior to harvesting cells for flow cytometric analysis.

Annexin V-FITC staining

To examine whether cells treated with nanoparticles underwent apoptosis, cells were stained with FITC-conjugated Annexin V (BD Biosciences, San Jose, CA). Cells were plated, treated with nanoparticles, and harvested with trypsin as described above. Cells were resuspended

in 100 µL of Annexin binding buffer (Life Technologies). Five µL of FITC Annexin V was added to each tube and the samples were incubated for 15 minutes in the dark at room temperature before adding an additional 400 µL of Annexin binding buffer. Fluorescence of bound FITC Annexin V was then detected by flow cytometry, excitation wavelength of 488 nm. All experimental conditions were performed in triplicate. As a positive control for apoptosis, a subset of wells were treated with 20 mM H_2O_2 in DMEM at the same time as nanoparticle treatment, 24 hours prior to harvest of cells for flow cytometric analysis.

LDH Assay

To further assess cell death by detecting cellular membrane damage, release of the cytosolic enzyme lactate dehydrogenase (LDH) into the culture medium was examined by colorimetric assay. Cells were plated and treated with nanoparticles as described above. After a 24-hour incubation, 50 µL of culture media was collected from each well and placed in a flat-bottom 96-well plate (BD Falcon). LDH activity was assessed using a commercially available kit (LDH Assay Kit, Sigma-Aldrich) according to manufacturer's instructions. Briefly, LDH Assay Substrate Solution, LDH Assay Cofactor Preparation, and LDH Assay Lysis Solution were added to samples and incubated at room temperature for 15-20 minutes. The absorbance was read on a microplate reader at 490 nm and 690 nm. Sample absorbance values were corrected by subtracting the background reading at 690 nm from the 490 nm reading. As a positive control for LDH release, cells were treated with a 1% solution of Triton X-100 (Sigma-Aldrich) in DMEM for 5 minutes to lyse all cells before collecting the supernatants. Sample absorbance values were normalized to the Triton positive control (considered as 0% cell viability) and untreated negative control (considered as 100% cell viability). All experimental conditions were performed in quadruplicate.

MTT Assay

To measure the metabolic activity of nanoparticle-treated cells, we used a commercially available MTT assay kit (Cayman Chemical, Ann Arbor, MI). In this assay, the tetrazolium dye, MTT, is reduced by mitochondrial NAD(P)H-dependent oxidoreductase enzymes to an insoluble purple crystal, formazan. Cells were plated and treated with nanoparticles as described above and incubated for 24 hours at 37°C prior to the assay. As a positive control for complete cell death, cells were treated with a 1% solution of Triton X-100 in DMEM for five minutes immediately before the assay was performed. After the incubation, cell culture media was removed and cells were washed once with PBS to prevent interaction of nanoparticles with the MTT reagent. Fresh cell culture media (200 µL) was added to each culture well before the addition of 10 µL of the MTT reagent. The cells were incubated for 3-4 hours at 37°C. The culture media/MTT reagent was removed and formazan crystals were dissolved with the provided MTT solvent. The solution was transferred to a flat-bottom 96-well plate and absorbance values were read using a microplate reader at 570 nm and 690 nm. Absorbance values were corrected by subtracting the background absorbance reading at 690 nm from the absorbance at 570 nm. To analyze and compare the data, absorbance values were normalized to the untreated control cells such that the untreated control represented 100% mitochondrial activity and an absorbance of 0 represented the absence of mitochondrial activity (i.e., 0%). All experimental conditions were performed in quadruplicate.

Cell proliferation

To assess the effects of nanoparticle exposure on proliferating cells, we compared cell proliferation of untreated cells with those treated with nanoparticles continuously over a 10 day period. The cells were seeded at a density of 5×10^4 cells/well so that they would reach confluence after approximately 10 days. Cells were plated in triplicate into 6-well tissue culture plates such that there were triplicate wells of each treatment to harvest and count daily for 10 days (total of 30

counts). The time at which cells were plated was considered time zero. One day after plating cells, cell culture media was changed and cells were treated with appropriate doses of nanoparticles. Nanoparticles were allowed to remain on cells for 48 hours, at which point cell culture media was changed and cells were re-treated with nanoparticles. Cells were re-treated with nanoparticles every 48 hours. Cells were counted daily using a Z2 Beckman Coulter Counter (Indianapolis, IN) and mean counts of triplicate wells were plotted versus time. Growth curves were normalized to the growth of untreated control cells such that the maximum count measured for the untreated control cells was considered 100% growth. The experiments performed using the antioxidant N-acetylcysteine (NAC, Sigma-Aldrich) was done similarly. NAC was dissolved in cell culture media and added to the cells at the same time as the first nanoparticle treatment and at every subsequent cell culture media change and nanoparticle retreatment. N-acetylcysteine (NAC, Sigma-Aldrich) was used at 10 mM. Optimal doses were determined based on preliminary experiments. After dissolving NAC in cell culture media, pH was adjusted to 7.4 using 1 N NaOH (Avantor Performance Materials, Center Valley, PA). After adding antioxidants and adjusting pH, cell culture media was filter sterilized before being added to cells.

Cell cycle analysis

In order to evaluate the effects of nanoparticles on cell cycle, proliferating cells were treated with nanoparticles and analyzed for DNA content by flow cytometry. Cells were plated in 6-well cell culture plates at a density between 5×10^4 and 1×10^5 cells/well. After 24-48 hour incubation, cells were treated with the appropriate doses of silver and digested silver. As was done for the growth curves, nanoparticles were left on the cells for 48 hours until media was changed on the cells and they were treated again with nanoparticles. Cells were grown for 5 days after plating until the untreated cells were approaching confluence but still proliferating. Once cells had

reached this point, they were harvested by trypsinization, washed with PBS, and suspended in 1 mL PBS. To fix cells, 4 mL absolute ethanol (Thermo Fisher Scientific, Waltham, MA) was slowly added to each sample while vortexing in order to minimize aggregation of cells and incubated at -20°C at least overnight and up to two weeks. Fixed cells were washed twice with PBS, suspended in 1 mL staining solution consisting of 0.1% Triton X-100 (Sigma-Aldrich), 100 µg/mL RNase A (Life Technologies), and 40 µg/mL propidium iodide (Sigma-Aldrich) in PBS. Cells were incubated in the dark at room temperature for 30 minutes and analyzed by flow cytometry at an excitation wavelength of 488 nm. All experimental conditions were performed in triplicate.

GSH assay

To determine the oxidative stress of cells, total and oxidized (GSSG) glutathione were measured using the GSH/GSSG-Glo™ Assay kit (Promega, Madison, WI). In this assay, glutathione is required for the reaction converting Luciferin-NT to luciferin (catalyzed by glutathione S-transferase, resulting in GSH-NT). The luciferin is then converted to light in a firefly luciferase reaction and light formed is thus dependent on the amount of glutathione. Total glutathione is measured by lysing cells, reducing any GSSG to reduced glutathione (GSH), and allowing the GSH to react with Luciferin-NT. GSSG is measured by blocking GSH with N-Ethylmaleimide and then reducing GSSG to GSH and allowing it to react with Luciferin-NT to eventually produce light. Both total GSH and GSSG were measured in order to determine the GSH/GSSG ratio. For the assay, cells were plated in 6-well cell culture plates at a density of 5×10^4 or 1×10^5 cells/well. Cells were allowed to adhere to the plate for one day prior to treatment with Ag NP. Cells were treated with the appropriate dose of pristine and digested Ag NP, centrifuged to promote contact of NP with cells, and incubated for 24 hours. Cells were then harvested by trypsinization, resuspended in cell culture media, washed once in HBSS, and resuspended in the

appropriate volume of HBSS for a cell density of 5×10^5 cells/ml. The assay was then performed according to the provided protocol, halving the volume of all reagents for each reaction. Briefly, 10 µl of cell suspension was added to each well along with 2.5 µL HBSS. Total Glutathione Lysis Reagent (12.5 µL) was prepared and added to wells to measure total glutathione while Oxidized Glutathione Lysis Reagent (12.5 µL) was added to a second set of wells to measure oxidized glutathione. The plate was shaken for 5 minutes before adding 25 µL Luciferin Generation Reagent to all wells. The plate was then incubated for 30 minutes at room temperature. After the incubation, Luciferin Detection Reagent (50 µL) was added to wells, the plate was incubated for 15 minutes at room temperature, and the luminescence was measured using a Packard TopCount (PerkinElmer, Waltham, MA). A standard curve was prepared at the same time with known concentrations of glutathione from 0-16 µM. The linear portion of the standard curve was used to determine the concentrations of GSH and GSSG measured. The Pierce BCA protein assay (Thermo Scientific) was used to report concentration based on protein. The assay was performed according to the provided protocol. Briefly, 100 µL of cell suspension was added to a test followed by 2 mL of the prepared working reagent (50 parts BCA Reagent A and 1 part BCA Reagent B). Tubes were incubated at 37°C for 30 minutes, cooled to RT, and absorbance was measured at 562 nm. A standard curve was prepared with known concentrations of BSA and used to calculate total protein in each treatment. GSH/GSSG ratios were calculated as follows (there are two moles of GSH per one mole of GSSG): GSH/GSSG = ([total glutathione] – [GSSG]*2) / [GSSG]. Each GSH assay was performed using three biological replicates of each treatment.

Results:

Silver Nanoparticle Synthesis

Ag NP were produced by reduction of silver ions to silver nanoparticles with borohydride using a previously reported synthesis.[24] These nanoparticles were stabilized with citrate. In order to simulate the *in vivo* gastrointestinal environment, Ag NPs were incubated sequentially with digestive enzyme solutions of pepsin (pH 2, stomach), pancreatin (pH 7, intestines), and bile extract (pH 7, intestines) for one hour each as has been previously described for titania and silica nanoparticles.[19] After incubations, particles were suspended in PBS and experiments were performed with both pristine and "digested" Ag.

Characterization of Silver Nanoparticles

Transmission electron microscopy (TEM) of the synthesized Ag NP revealed largely spherical particles with an average diameter of 23 ± 8 nm (Figure 1A). Zeta potential of pristine and digested Ag particles was compared over a range of pH values from neutral to acidic pH (Figure 1B). At a pH of 7, both pristine and digested Ag NP have negative surface charge, but the zeta potential of the pristine silver is more strongly negative than that of the digested Ag (-46.6 ± 2.7 mV vs. -26.0 ± 2.2 mV). As the pH decreases, the zeta potential for the Ag NP approaches 0 mV, and this happens at approximately pH 2 for pristine Ag but approximately pH 3 for digested Ag. Thus, while the trend for the zeta potential is the same for pristine and digested Ag NP, the actual values differ. Infrared spectra for pristine and digested Ag reveal differences in the surface of pristine and digested Ag NP (Figure 1C). The peak at 1673 cm^{-1} in the digested Ag NP spectrum is likely due to protein adsorption, specifically β-sheet structures.[25] Raman spectra differ between the pristine and digested Ag as well (Figure 1D). XPS spectra reveal some differences in the elements on the surface of the digested and pristine particles (Figure 1E). Specifically, there are more defined carbon and oxygen peaks for pristine Ag while there are much larger sodium, chlorine, phosphorus, and nitrogen peaks for digested Ag (Figure 2).

To determine the extent of Ag NP solubility in cell culture medium, the Ag ion concentration in solution was determined after 0, 24, and 48-hour incubation in cell culture media (Figure 3). In experiments with cells, 48 hours was the maximal duration of Ag NP exposure in the same culture media. After 48 hours, cell media would be changed and new Ag NP added to the cells. Thus, Ag NP solubility over this time frame was most relevant to later experiments. Initial concentration of Ag ions in solution immediately after dispersal of Ag NP in media was similar for pristine and digested Ag (0.32 and 0.36 ppm, respectively). The concentration of digested Ag ions in solution did increase to 0.57 ppm after 24 hours in media, but decreased again by 48 hours (to 0.20 ppm), suggesting precipitate formation. The concentration of Ag ions in solution for the pristine Ag NP decreased after 24 and 48-hour incubation (to 0.27 and then 0.16 ppm, respectively) as compared to the initial concentration. These experiments show no drastic difference in availability of Ag ions between pristine and digested Ag. Also, the concentration of free Ag ions available to interact with cells is small in comparison to the concentration of Ag NP (1250 ppm).

Cell Internalization of Silver Nanoparticles

It has been shown that Ag NP are internalized by cells, including intestinal epithelial cells.[16] To confirm this in the C2BBe1 intestinal epithelial cell model (a sub-clone of Caco-2 cells), cells were treated with Ag NP for 24 hours and fixed for transmission electron microscopy. TEM revealed that these cells do internalize both pristine and digested Ag NP (Figure 4). The internalized particles were not found in cell nuclei and were not contained within clear vesicles, but seemed to be free agglomerates in the cell cytoplasm. The digested Ag NP were in large agglomerates within cells which were likely formed prior to internalization based on DLS measurements showing an average particle diameter of 90.9 ± 2.8 nm prior to digestion and 346 ± 105 nm after digestion.

Silver Nanoparticle Toxicity in Proliferating Cells

To examine toxicity of nanoparticles in cells, Sytox Red staining of DNA in cells with compromised membranes and analysis by flow cytometry was used to detect necrotic cell death. Annexin V FITC was used to label apoptotic cells for detection by flow cytometry. Colorimetric detection of lactate dehydrogenase (LDH) released from cells was used as a measure of membrane damage. Finally, the MTT assay was used as a measure of mitochondrial activity in cells. Cells plated at low density were treated with 0.25 μg/cm^2 pristine or 0.5 μg/cm^2 digested Ag NP for 24 hours before performing each of these assays. No apoptosis and minimal increase in LDH release was detected (Figure 5B,C). However, the Sytox Red staining detected 20% induction of necrotic cell death and the MTT assay detected 80% reduction in cell metabolic activity (Figure 5A,D).

Silver Nanoparticle Inhibition of Cell Proliferation

Growth curves were performed to examine the effects of Ag NP on proliferating cells. Cells were plated at low density and allowed to adhere to the plate overnight. After 24 hours, cells were treated with Ag NP and subsequently treated again with Ag NP every 48 hours when cell culture media was changed. A subset of cells were counted each day. Untreated cells grew and reached a plateau, as expected (Figure 6A). However, a dose of 0.25 μg/cm^2 pristine Ag and above initially killed some cells and then induced complete inhibition of cell proliferation over the course of the 10 days (Figure 6A). Cells treated with digested Ag show a similar inhibition of cell proliferation, but only at a dose of 0.5 μg/cm^2 digested Ag and above (Figure 6B).

Since we saw this inhibition of cell proliferation with Ag NP, we decided to look at the effects of other food-relevant NP on cell growth. We have previously shown minimal acute toxicity of SiO_2, TiO_2, and ZnO NP to C2BBe1 cells,[19] similar to the toxicity observed in this study with Ag NP (Figure 6C-E). Growth curves were performed with SiO_2, TiO_2, and ZnO NP from 1 μg/cm^2

up to a 10 μg/cm^2 dose, as was used in the toxicity studies. SiO_2 and TiO_2 induced dose-dependent growth inhibition, with only partial inhibition of cell proliferation at the highest dose (Figure 6C, D). ZnO NP also induced dose-dependent growth inhibition with complete inhibition of cell proliferation at a dose of 10 μg/cm^2 (Figure 6E). Thus, Ag NP are not the only food-relevant NP that can inhibit cell proliferation. However, since Ag NP were able to completely inhibit cell proliferation at a dose 40 times lower than ZnO (Figures 6A,E), it is clear that the action of the Ag NP is unique. Treatment of cells with zeolite particles of sizes 40, 200, and 2000 nm at a dose of 10 μg/cm^2 induced partial inhibition of cell proliferation (Figure 6F), so the inhibition of proliferation observed with SiO_2 and TiO_2 treatment may be more of a mechanical effect than an effect specific to the particles.

To further investigate the cell proliferation inhibition induced by Ag NP, cell cycle analysis was performed using propidium iodide staining and flow cytometry analysis. The cell cycle analysis was performed on proliferating cells and the experiment was set up similarly to the growth curve experiments. Cells were plated at low density and allowed to proliferate for five days. After adhering overnight, cells were treated with Ag NP and then treated again two days later when cell culture media was changed. Cell cycle analysis revealed an increase in G2/M phase cells paired with a decrease in G0/G1 phase cells at a dose of 0.25 μg/cm^2 pristine Ag (Figure 7A) and doses of 0.25 ug/cm^2 and 0.5 ug/cm^2 digested Ag (Figure 7B). The histograms clearly show the increase in G2/M phase cells and decrease in G0/G1 phase cells after treatment with 0.25 μg/cm^2 pristine Ag (Figure 7D) or 0.5 ug/cm^2 digested Ag (Figure 7E) over untreated cells (Figure 7C). This increase in G2/M phase cells at the doses at which we observed complete inhibition of cell proliferation suggests a cell cycle arrest at the G2/M phase.

Role of Oxidative Stress in Silver Nanoparticle-Induced Inhibition of Cell Proliferation

It has previously been shown that Ag NP can exert toxicity in various cell types through induction of oxidative stress.[12, 16, 17, 26] In order to investigate the role of oxidative stress in Ag NP-induced inhibition of cell proliferation, glutathione levels were measured in cells. In order to perform the glutathione assay, cells were plated at low density, allowed to adhere to plates overnight, and treated with Ag NP for 24 hours which was the time at which the greatest differences in glutathione levels were observed. No difference in GSH/GSSG ratio was measured after treatment of proliferating cells with Ag NP for 4 days (data not shown). After 24-hour treatment of cells with Ag NP, reduced glutathione (GSH) and oxidized glutathione (GSSG) levels were measured in cells and were reported along with the GSH/GSSG ratio (Figure 8). Despite a slight increase in GSH within cells (Figure 8A), GSSG increased significantly more (Figure 8B), leading to a significant and repeatable decrease in the GSH/GSSG ratio after treatment of cells with pristine and digested Ag NP (Figure 8C). This suggests that Ag NP treatment does induce oxidative stress in intestinal epithelial cells.

To determine if oxidative stress is causing the inhibition of cell proliferation observed here, the antioxidant N-acetylcysteine (NAC) was used to protect against induction of oxidative stress. NAC is a precursor of glutathione which helps to neutralize reactive oxygen species in cells.[27] Growth curves were performed as previously described with the addition of the antioxidant into the cell culture media the entire time the cells were treated with Ag NP. Cells were treated with a 0.25 $\mu g/cm^2$ dose of pristine Ag or a 0.5 $\mu g/cm^2$ dose of digested Ag to induce complete inhibition of cell proliferation. Thus, the curve with no added antioxidant displays complete inhibition of cell proliferation (Figure 9A). When cells were treated with NAC in addition to the Ag NP, there was significant protection from the Ag NP-induced proliferation inhibition and cells treated with Ag NP appear to be proliferating almost as quickly as the untreated cells (Figure 9B). GSH assays

performed on cells treated for 24 hours with Ag and NAC showed very little change in GSH/GSSG ratio after Ag NP treatment, suggesting no induction of oxidative stress (Figure 9C). Because NAC can complex with Ag and chelate Ag ions, it is unclear if the protection of cells by NAC from inhibition of proliferation induced by Ag NP is due to the antioxidant activity of NAC within cells or the chelation of Ag ions before they enter the cells. To address this complexation of Ag with NAC, cells were pretreated with NAC for 1 hour and NAC-containing media was removed from cells before treatment of cells with Ag NP. Growth curves showed no difference in growth of Ag NP-treated cells with or without pretreatment with NAC within 5 days of Ag NP treatment (Figure 10A). In two out of three GSH assays performed after 1 hour NAC pretreatment and 24-hour Ag NP treatment, the GSH/GSSG ratio of the pretreated cells was slightly higher than that of the cells not treated with NAC (Figure 10B). In the third experiment, no difference was observed after NAC pretreatment (Figure 10C). Thus, NAC pretreatment may be slightly protective from induction of oxidative stress, but it does not play a large role. Furthermore, the complete protection from oxidative stress and inhibition of cell proliferation that NAC conferred in the presence of Ag NP is likely due to complexation of NAC with Ag ions.

Cytotoxicity of Silver Nanoparticles in Confluent Cells

To examine toxicity of Ag NP in confluent cells, the same four toxicity assays were run. Confluent cells were treated with 10 $\mu g/cm^2$ pristine or digested Ag NP for 24 hours before performing each of these assays. No decrease in cell viability after Ag NP treatment was detected with these assays (Figure 11). There was a slight decrease in mitochondrial activity after treatment with pristine and digested Ag NP but it was not significant (Figure 11). The LDH assay was not performed with digested Ag as the digestive enzymes were previously observed to interfere with

the assay.[19] Measurement of GSH/GSSG after 24-hour treatment of confluent cells with 0.25 μg/cm^2 to compare to proliferating cells revealed no change in the ratio (Figure 8D).

Discussion

Cell internalization of Ag NP:

In order to study the intestinal epithelium, we used the C2BBe1 cell line. These cells were cloned from the Caco-2 cell line for more homogeneous brush border (microvilli) formation. The cells have been shown to express the same brush border proteins found *in vivo* and thus form a good model of normal intestinal epithelium.[28] We observed by TEM that Ag nanoparticles were internalized by confluent C2BBe1 cells after 24-hour exposure to 50 μg/mL (10 μg/cm^2) Ag NP and that these internalized nanoparticles localized to the cytoplasm of cells (Figure 4). Internalization of Ag NP by cells is likely to contribute to and may be necessary for NP cytotoxicity. *In vivo,* transport of NP through intestinal epithelial cells will allow NP to enter the circulation and the rest of the body, allowing the NP to induce effects throughout the body. Internalization of Ag NP by Caco-2 cells has previously been shown by TEM with 15 μg/mL of Ag NP < 100 nm[16] and 20 μg/mL of 20 nm Ag NP.[14] Based on the doses used in these studies, it is likely that uptake of Ag NP would be apparent within our cells at even lower doses than what we used for the TEM studies (50 μg/mL). Many researchers have found Ag NP to localize in the cytoplasm of cells[16] which is also consistent with what we observed.

Proliferating cells:

Exposure of proliferating cells (in our study defined as < 10,000 cells/cm^2) to Ag NP at a dose of 0.25 μg/cm^2 (1.25 μg/mL) for 24 hours led to necrotic cell death in 20% of cells and an 80% decrease in metabolic activity (Figure 5). This induction of necrotic cell death is consistent

with several previous studies of Ag NP treatment in Caco-2 cells.[17, 29] The decrease in metabolic activity is also in agreement with several papers in Caco-2 cells treated with Ag NP.[14, 16, 17, 29, 30] Treatment of proliferating cells with Ag NP for 24 hours decreased the GSH/GSSG ratio to less than half the level in untreated cells, indicating oxidative stress (Figure 8). Other studies in Caco-2 cells have shown induction of oxidative stress by detection of ROS species production[17, 31] and gene expression studies showed upregulation of genes involved in oxidative stress in the Caco-2/M cell model.[32] However, some studies have not detected ROS formation in Caco-2 cells.[14, 15, 29] This is likely due to lower sensitivity of ROS detection over the GSH/GSSG ratio. For instance, a study in Caco-2 cells treated with Ag NP < 100 nm did not observe an increase in ROS production but did determine that there was oxidative stress due to a decrease in total cellular GSH.[16] Alternatively, these studies may not have detected oxidative stress due to the use of Ag NP synthesized differently or more confluent cells which may be less sensitive to Ag NP treatment. In addition to acute toxicity to cells, oxidative stress can inhibit cell proliferation. Ag NP treatment of proliferating cells at 0.25 μg/cm^2 for 96 hours induced G2/M phase cell cycle arrest (increase in G2/M phase cells from 23 to 49%) as determined by propidium iodide staining and flow cytometric analysis (Figure 7). To our knowledge, this is the first paper reporting cell cycle arrest in an intestinal epithelial cell model although G2/M phase cell cycle arrest has been reported previously in other cell models including lung epithelial cells.[11, 33-35] There is a DNA damage checkpoint at the end of the G2 phase of the cell cycle and thus G2/M phase arrest may be allowing cells with DNA damage time to repair their DNA. This model of DNA damage response has previously been proposed as the reason for cell cycle arrest after Ag NP treatment.[11, 35] Cell proliferation as measured by growth curves was completely inhibited with 0.25 μg/cm^2 treatment of cells with Ag NP (Figure 6). Although using other methods to detect cell proliferation, several other studies have

also detected a decrease in cell proliferation in both Caco-2 cells[14] as well as other cell models.[36, 37] Because we observed complete inhibition of cell proliferation but not did not observe all cells arrested in the G2/M phase, this would suggest that some cells are being arrested in other phases of the cell cycle. Alternatively, the observed inhibition may be due to continued cell death while some cells are still proliferating. Since the majority of the cell death was observed to occur within the first several days of the growth curve experiments (Figures 5,6), it is more likely that cells are being arrested at various stages of the cell cycle. This oxidative stress response leading to cell cycle arrest and inhibition of cell proliferation is depicted in Figure 12.

Treatment of cells with ZnO NP at a dose of 10 μg/cm^2 also inhibited cell proliferation completely. This inhibition of cell proliferation by ZnO NP is consistent with previous studies.[38, 39] Some studies have also linked ZnO NP-induced inhibition of cell proliferation to induction of oxidative stress.[39] Treatment of cells with 10 μg/cm^2 SiO_2 or TiO_2 NP only partially inhibited cell proliferation. Treatment of cells with 40, 200, and 2000 nm zeolite particles also partially inhibited cell proliferation. This suggests that the partial inhibition induced by SiO_2 and TiO_2 NP is likely not specific to the NP but a more general mechanical effect induced by treatment with any particles.

In the existing literature on Ag NP exposure in intestinal epithelial cells, most studies have been performed on confluent cells. Since proliferating cells are not surrounded by cells on all sides, each cell has a greater surface area exposed to Ag NP. Also, because of the many cell processes needed for replication, proliferating cells are more metabolically active and any damage induced by Ag NP may be more quickly apparent in proliferating cells than it would be in confluent cells. Although little literature exists on the effects of Ag NP in proliferating cells, it has been shown that proliferating Caco-2 cells were more sensitive to Ag NP-induced toxicity and differentiated

Caco-2 cells required higher doses of Ag NP to induce the same cytotoxic response.[17, 40] It is well known in models of biological stress such as ionizing radiation that proliferating cells are more sensitive to toxic agents. The radiosensitivity of cells generally decreases with increasing cell differentiation. Thus, the cells that are actively proliferating are much more sensitive to irradiation.[41] This is due to induction of DNA damage which leads to either cell cycle arrest to allow time for DNA repair or induction of apoptosis.[42] Thus, proliferating cells are expected to be more sensitive to toxic agents due to their greater metabolic activity. Proliferating cells are also being exposed to more nanoparticles/cell than confluent cells receiving the same dose of nanoparticles. Thus, this may also increase their sensitivity to NP treatment.

N-acetylcysteine is an antioxidant that is able to reduce free radicals due to its thiol group. It can also be used by cells to synthesize more glutathione and thus give cells greater antioxidant capacity. Because of these properties, NAC has been used frequently in experiments to rescue toxicity in order to show that Ag NP (or other stressors) are mediating their effects through an oxidative stress response. In our studies, exposure of cells to 10 mM NAC along with 1.25 μg/mL 23 nm Ag NP was protective against Ag NP-induced inhibition of cell proliferation (Figure 9). However, because of its thiol group, NAC can also bind to and interact with Ag ions. Thus, it is possible that the apparent rescue of Ag NP-mediated inhibition of cell proliferation in our system is due to complexation of NAC with Ag ions rather than protection via its antioxidant properties. Pretreatment of cells with 10 mM NAC for 1 hour and removal of NAC before exposure of cells to 1.25 μg/mL Ag NP to eliminate the possibility of NAC complexation with Ag ions was unable to protect against Ag NP-induced inhibition of cell proliferation and did not affect the induction of oxidative stress in cells (Figure 10). Thus, it is likely that NAC is complexing with Ag ions and preventing them from mediating toxicity against cells rather than protecting cells from oxidative

stress internally. This response is depicted in Figure 12B. In agreement with our experiments, in *C. elegans,* NAC was able to rescue growth inhibition induced by Ag NP treatment and by $AgNO_3$ and they concluded that chelation of Ag ions by NAC was mainly responsible for the effects of NAC.[43] Several studies have pretreated cells with NAC and then removed NAC before treating cells with Ag NP to eliminate the possibility of complexation of Ag ions with NAC, and these studies observed partial protection of NAC pretreatment from Ag NP-induced toxicity, contrary to our results. However, one study performed in Caco-2 cells observed NAC protection from upregulation of genes involved in oxidative stress,[16] which is likely more sensitive than cell growth. Another study which pretreated A549 cells with NAC showed that NAC could partially protect cells from Ag NP-induced decreases in cell viability and death and induction of ROS, but was not protective against cell cycle arrest.[13] They suggest that this is because the cell cycle effects are the result of an oxidative stress-independent pathway. However, since our studies in proliferating cells also did not reveal a decrease in cell proliferation after NAC pretreatment, this could be a difference between proliferating cells (used for the cell cycle experiments) and confluent cells (used for viability and ROS experiments). Alternatively, this could be due to a difference in Ag NP used (40-90 nm in diameter vs. 23 nm).

There has been some debate as to whether the toxicity of Ag NP is mediated through the nanoparticles themselves or through Ag ions arising from dissolution of the Ag NP. It is known that Ag NP will dissolve to some extent and release silver ions into solution. One study determined that 70% of citrate-stabilized nanoparticles will dissolve after 3000 hours at 37°C, but only 14% will dissolve at 25°C.[44] Our experiments with NAC suggest that since complexation of NAC with Ag ions can completely inhibit cell proliferation and induction of oxidative stress, most of the Ag NP toxicity is likely mediated through Ag ions. Many studies have looked at toxicity both Ag NP

and Ag ions and have seen mixed results. Several studies have determined that Ag NP toxicity is mediated through Ag ions, in agreement with us. A study in Caco-2/M cells observed similar changes in gene expression after treating cells with 20, 34, 61, and 113 nm Ag NP and 1.5 µg/mL Ag ions (from $AgNO_3$, concentration representative of the Ag ions in solution and concluded that the toxicity of Ag NP is mediated through Ag ions.[32] A study using 90 nm Ag NP in Caco-2 cells showed that 2.18% of the Ag of a 15 µg/mL suspension of Ag NP was in the form of Ag ions when initially suspended in cell culture media. After 24 hours, the Ag ions in solution were 3.47% of the total Ag. These amounts corresponded to 3.57 µM Ag ions at 0 hours and 4.82 µM at 24 hours.[16] They compare these amounts of Ag to a study that showed that 5 µM $AgNO_3$ could induce oxidative stress measured by ROS production and GSH reduction as well as cytotoxicity in human skin fibroblasts.[45] Thus, since these comparable amounts of Ag ions are causing similar toxicity and oxidative stress in cells, they conclude that Ag ions are likely mediating toxicity of Ag NP. However, since Ag NP are internalized by cells, there will be some ion dissolution internally which will add to Ag NP toxicity. However, a study in Caco-2 cells treated cells with supernatants from 20 nm Ag NP that were incubated for 24 hours in cell culture media. This supernatant, which should have contained all dissolved Ag ions, caused only slight decrease in DAPI staining at a concentration of 100 µg/mL. Thus, they concluded that Ag NP were physically required to cause the cytotoxicity observed.[17] This may have to do with the amount of Ag ions that dissolve in solution versus those dissolving once Ag NP have been internalized by cells. A study of *in vitro* digestion of Ag NP also used Ag ions ($AgNO_3$) and saw that after intestinal digestion, $AgNO_3$ would form some Ag NP.[46] Thus, *in vivo*, even if Ag NP dissolve to some extent in the stomach or digestion process, it is likely that they will reach the intestinal epithelium as Ag NP, although once they are in cells, their toxicity may be mediated through Ag ions. An *in vivo* study

administering solutions of Ag NP or Ag ions orally to rats for 28 days found that the concentrations of Ag in tissues were correlated to the amount of Ag ions in the initial solution, suggesting that Ag ions are the major species transported across the intestine and into the rest of the body.[9] Also, they found Ag NP in tissue even of rats treated with Ag ions, again suggesting that Ag ions can form Ag NP *in vivo*. A similar 28-day study orally administering Ag NP or Ag acetate to rats observed Ag NP containing selenium and sulfur in animals administered the Ag NP as well as the Ag acetate, suggesting that Ag NP dissolve and then they may form NP in some tissues.[47] Thus, even if Ag NP are dissolving *in vivo*, there may still be formation of Ag NP once these ions are distributed to the tissue.

It is well-known that NP can adsorb proteins to their surface.[48] This protein corona will then determine the biological interactions of NP. Orally ingested NP will be exposed to many proteins in the digestive tract which may be incorporated into their protein coronas and thus change their interactions with cells. To mimic *in vivo* digestion, we incubated nanoparticles with synthetic digestive enzyme solutions representing stomach and intestines. These digested Ag NP required a slightly higher dose (0.5 μg/cm^2) to cause the same inhibition of proliferation as the pristine Ag NP (0.25 μg/cm^2; Figure 6). We are hypothesizing that this is due to protection of the digested Ag NP from dissolution because of increased proteins on the surface of the NP after digestion. However, it is also possible that the large agglomerates formed by digested Ag, as visualized by TEM (Figure 4B), impeded interaction with and internalization by cells, thus leading to a decreased effect. Other studies have also looked at the effects of Ag NP subjected to an *in vitro* digestion process. In a study in Caco-2 cells, digested 7 nm Ag NP showed toxicity detected by decreased impedance measurements of proliferating cells. The toxicity of the digested Ag NP in comparison to that of undigested Ag NP was delayed by approximately 12 hours and required a

dose of 10 µg/mL digested Ag NP whereas the undigested Ag NP induced toxicity at a dose of 5 µg/mL.[40] They attribute this to lower bioavailability and silver ion release of Ag NP after digestion. However, they observed similar toxicity after 24-hour exposure to undigested and digested Ag NP at concentrations of 15 µg/mL and above in proliferating cells and at 25 µg/mL in differentiated cells using the CellTiter Blue assay to measure metabolic activity of cells and DAPI staining to measure cell number. The digestive enzyme solution itself caused a decrease in metabolic activity in differentiated but not proliferating cells at an amount corresponding to 25 µg/mL nanoparticles. At the digestion fluid mixture amount corresponding to 50 µg/mL NP, cell number begins to decrease.[40] In this study, we observed that pristine and digested Ag NP were not toxic to confluent cells at 40 µg/mL after 24 hours. However, in proliferating cells, we observed toxicity and inhibition of proliferation at doses of 1.25 µg/mL for pristine Ag NP and 2.5 µg/mL for digested Ag NP. Thus, we show lower Ag NP toxicity in confluent cells than Bohmert et al. did in differentiated cells, but greater toxicity in proliferating cells.[40] The differences on proliferating cells may be due to plating at different cell densities. For assays with proliferating cells, we plated cells at a factor 10-20 times below confluence whereas Bohmert et al. plated cells for impedance assays approximately 5 times below confluence.[40]

Confluent cells:

To compare confluent cells (>100,000 cells/cm^2) to the studies in proliferating cells, toxicity assays were performed after 24-hour treatment of cells with 10 µg/cm^2 Ag NP. Sytox Red staining, Annexin V FITC staining, the LDH assay, and the MTT assay revealed no cell death or decrease in metabolic activity induced by Ag NP treatment (Figure 11). We also did not observe a change in GSH/GSSG ratio in confluent cells after treatment with 0.25 µg/cm^2 Ag NP, suggesting that a higher dose of Ag NP would likely be required to induce oxidative stress in confluent cells.

In the literature, Ag NP have generally induced toxicity in cells based on similar assays to the ones we employed, but there is some variation in the dose at which toxicity is observed and the extent of the toxicity. However, there are several studies in intestinal epithelial cell models consistent with our results.[15, 17, 32] Other studies in Caco-2 cells disagree with us and observed toxicity at Ag NP doses lower than those we used.[14, 16, 29, 30] However, it is likely that these differences are due to studies being performed at lower cell densities (between 10,000 and 100,000 cells/cm^2) so that cells may be more sensitive to NP treatment[16, 30] and differences in the Ag NP used in the studies.[14, 29] The lack of toxicity in confluent cells may be due to their decreased sensitivity to cell stressors (from decreased metabolic activity) and a decreased exposure of each cell to nanoparticles. Also, confluent cells are more tightly packed into cell culture plates so that each cell has a smaller available surface area to interact with Ag NP. These cells also form intercellular junctions that prevent transport of Ag NP between and underneath cells.

***In vivo* implications:**

The current study has implications for proliferation of intestinal epithelium *in vivo*. The stem cells at the base of intestinal crypts are constantly proliferating in order to renew the intestinal epithelium. If ingested Ag NP are able to slow this proliferation, this may seriously impair the epithelial barrier function. To date, *in vivo* studies with orally administered Ag NP have shown damage to the microvilli of intestinal epithelial cells and intestinal glands in mice,[49] indications of slight liver damage,[50] and changes in intestinal mucus composition and greater release of mucus granules from Goblet cells along with cell shedding at the tips of villi in the ileum,[10] but no studies known to us have reported impairment of the epithelial barrier. Inhibition of stem cell proliferation by Ag NP may have more serious consequences in disease intestines including inflammatory

bowel disease where the epithelial barrier is already compromised. Therefore, Ag NP ingestion needs to be investigated in intestinal disease models.

References

1. Abou El-Nour, K. M. M.; Eftaiha, A. a.; Al-Warthan, A.; Ammar, R. A. A., Synthesis and applications of silver nanoparticles. *Arabian Journal of Chemistry* **2010**, 3, 135–140.

2. Alexander, J. W., History of the medical use of silver. *Surg Infect (Larchmt)* **2009**, 10, 289-92.

3. The Project on Emerging Nanotechnologies Consumer Products Inventory. http://www.nanotechproject.org/inventories/consumer/ (June 20, 2013),

4. Kim, J. S.; Kuk, E.; Yu, K. N.; Kim, J. H.; Park, S. J.; Lee, H. J.; Kim, S. H.; Park, Y. K.; Park, Y. H.; Hwang, C. Y.; Kim, Y. K.; Lee, Y. S.; Jeong, D. H.; Cho, M. H., Antimicrobial effects of silver nanoparticles. *Nanomedicine* **2007**, 3, 95-101.

5. Desai, M. P.; Labhasetwar, V.; Amidon, G. L.; Levy, R. J., Gastrointestinal uptake of biodegradable microparticles: effect of particle size. *Pharm Res* **1996**, 13, 1838-45.

6. Jani, P.; Halbert, G. W.; Langridge, J.; Florence, A. T., Nanoparticle uptake by the rat gastrointestinal mucosa: quantitation and particle size dependency. *J Pharm Pharmacol* **1990**, 42, 821-6.

7. Awaad, A.; Nakamura, M.; Ishimura, K., Imaging of size-dependent uptake and identification of novel pathways in mouse Peyer's patches using fluorescent organosilica particles. *Nanomedicine* **2012**, 8, 627-36.

8. Platonova, T. A.; Pridvorova, S. M.; Zherdev, A. V.; Vasilevskaya, L. S.; Arianova, E. A.; Gmoshinski, I. V.; Khotimchenko, S. A.; Dzantiev, B. B.; Popov, V. O.; Tutelyan, V. A., Identification of silver nanoparticles in the small intestinal mucosa, liver, and spleen of rats by transmission electron microscopy. *Bull Exp Biol Med* **2013**, 155, 236-41.

9. van der Zande, M.; Vandebriel, R. J.; Van Doren, E.; Kramer, E.; Herrera Rivera, Z.; Serrano-Rojero, C. S.; Gremmer, E. R.; Mast, J.; Peters, R. J.; Hollman, P. C.; Hendriksen, P. J.; Marvin, H. J.; Peijnenburg, A. A.; Bouwmeester, H., Distribution, elimination, and toxicity of silver nanoparticles and silver ions in rats after 28-day oral exposure. *ACS Nano* **2012**, 6, 7427-42.

10. Jeong, G. N.; Jo, U. B.; Ryu, H. Y.; Kim, Y. S.; Song, K. S.; Yu, I. J., Histochemical study of intestinal mucins after administration of silver nanoparticles in Sprague-Dawley rats. *Arch Toxicol* **2010**, 84, 63-9.

11. AshaRani, P. V.; Mun, G. L. K.; Hande, M. P.; Valiyaveettil, S., Cytotoxicity and Genotoxicity of Silver Nanoparticles in Human Cells. *ACS Nano* **2009**, 3, 279-290.

12. Eom, H. J.; Choi, J., p38 MAPK activation, DNA damage, cell cycle arrest and apoptosis as mechanisms of toxicity of silver nanoparticles in Jurkat T cells. *Environ Sci Technol* **2010**, 44, 8337-42.

13. Chairuangkitti, P.; Lawanprasert, S.; Roytrakul, S.; Aueviriyavit, S.; Phummiratch, D.; Kulthong, K.; Chanvorachote, P.; Maniratanachote, R., Silver nanoparticles induce toxicity in A549 cells via ROS-dependent and ROS-independent pathways. *Toxicol In Vitro* **2013**, 27, 330-8.

14. Sahu, S. C.; Roy, S.; Zheng, J.; Yourick, J. J.; Sprando, R. L., Comparative genotoxicity of nanosilver in human liver HepG2 and colon Caco2 cells evaluated by fluorescent microscopy of cytochalasin B-blocked micronucleus formation. *J Appl Toxicol* **2014**, 34, 1200-8.

15. Abbott Chalew, T. E.; Schwab, K. J., Toxicity of commercially available engineered nanoparticles to Caco-2 and SW480 human intestinal epithelial cells. *Cell Biol Toxicol* **2013**, 29, 101-16.

16. Aueviriyavit, S.; Phummiratch, D.; Maniratanachote, R., Mechanistic study on the biological effects of silver and gold nanoparticles in Caco-2 cells--induction of the Nrf2/HO-1 pathway by high concentrations of silver nanoparticles. *Toxicol Lett* **2014**, 224, 73-83.

17. Bohmert, L.; Niemann, B.; Thunemann, A. F.; Lampen, A., Cytotoxicity of peptide-coated silver nanoparticles on the human intestinal cell line Caco-2. *Arch Toxicol* **2012**, 86, 1107-15.

18. L., C. M.; Yee, A. T., Intestinal redox biology and oxidative stress. **2012**, 23, 729–737.

19. McCracken, C.; Zane, A.; Knight, D. A.; Dutta, P. K.; Waldman, W. J., Minimal intestinal epithelial cell toxicity in response to short- and long-term food-relevant inorganic nanoparticle exposure. *Chem Res Toxicol* **2013**, 26, 1514-25.

20. Mandalari, G.; Faulks, R. M.; Rich, G. T.; Lo Turco, V.; Picout, D. R.; Lo Curto, R. B.; Bisignano, G.; Dugo, P.; Dugo, G.; Waldron, K. W.; Ellis, P. R.; Wickham, M. S., Release of protein, lipid, and vitamin E from almond seeds during digestion. *J Agric Food Chem* **2008**, 56, 3409-16.

21. Glahn, R. P.; Wien, E. M.; Van Campen, D. R.; Miller, D. D., Caco-2 cell iron uptake from meat and casein digests parallels in vivo studies: use of a novel in vitro method for rapid estimation of iron bioavailability. *J Nutr* **1996**, 126, 332-9.

22. Reboul, E.; Richelle, M.; Perrot, E.; Desmoulins-Malezet, C.; Pirisi, V.; Borel, P., Bioaccessibility of carotenoids and vitamin E from their main dietary sources. *J Agric Food Chem* **2006**, 54, 8749-55.

23. Connolly, M. L.; Lovegrove, J. A.; Tuohy, K. M., In vitro evaluation of the microbiota modulation abilities of different sized whole oat grain flakes. *Anaerobe* **2010**, 16, 483-8.

24. R. Christopher Doty, ‡; T. Robert Tshikhudo; Mathias Brust, a.; David G. Fernig*, Extremely Stable Water-Soluble Ag Nanoparticles. *Chemistry of Materials* **2005**, 17, 4630-4635.

25. Roach, P.; Farrar, D.; Perry, C. C., Surface tailoring for controlled protein adsorption: effect of topography at the nanometer scale and chemistry. *J Am Chem Soc* **2006**, 128, 3939-45.

26. AshaRani, P. V.; Mun, G. L. K.; Hande, M. P.; Valiyaveettil, S., Cytotoxicity and Genotoxicity of Silver Nanoparticles in Human Cells. *ACS Nano* **2008**, 3, 279-290.

27. Zafarullah, M.; Li, W. Q.; Sylvester, J.; Ahmad, M., Molecular mechanisms of N-acetylcysteine actions. *Cell Mol Life Sci* **2003**, 60, 6-20.

28. Peterson, M. D.; Mooseker, M. S., Characterization of the enterocyte-like brush border cytoskeleton of the C2BBe clones of the human intestinal cell line, Caco-2. *J Cell Sci* **1992**, 102 (Pt 3), 581-600.

29. Kaiser, J. P.; Roesslein, M.; Diener, L.; Wick, P., Human health risk of ingested nanoparticles that are added as multifunctional agents to paints: an in vitro study. *PLoS One* **2013**, 8, e83215.

30. Song, Y.; Guan, R.; Lyu, F.; Kang, T.; Wu, Y.; Chen, X., In vitro cytotoxicity of silver nanoparticles and zinc oxide nanoparticles to human epithelial colorectal adenocarcinoma (Caco-2) cells. *Mutat Res* **2014**, 769, 113-8.

31. Martirosyan, A.; Bazes, A.; Schneider, Y. J., In vitro toxicity assessment of silver nanoparticles in the presence of phenolic compounds--preventive agents against the harmful effect? *Nanotoxicology* **2014**, 8, 573-82.

32. Bouwmeester, H.; Poortman, J.; Peters, R. J.; Wijma, E.; Kramer, E.; Makama, S.; Puspitaninganindita, K.; Marvin, H. J.; Peijnenburg, A. A.; Hendriksen, P. J., Characterization of translocation of silver nanoparticles and effects on whole-genome gene expression using an in vitro intestinal epithelium coculture model. *ACS Nano* **2011**, 5, 4091-103.

33. Asharani, P.; Sethu, S.; Lim, H. K.; Balaji, G.; Valiyaveettil, S.; Hande, M. P., Differential regulation of intracellular factors mediating cell cycle, DNA repair and inflammation following exposure to silver nanoparticles in human cells. *Genome Integr* **2012**, 3, 2.

34. Lee, Y. S.; Kim, D. W.; Lee, Y. H.; Oh, J. H.; Yoon, S.; Choi, M. S.; Lee, S. K.; Kim, J. W.; Lee, K.; Song, C. W., Silver nanoparticles induce apoptosis and G2/M arrest via PKCzeta-dependent signaling in A549 lung cells. *Arch Toxicol* **2011**, 85, 1529-40.

35. Peng, H.; Zhang, X.; Wei, Y.; Liu, W.; Li, S.; Yu, G.; Fu, X.; Cao, T.; Deng, X., Cytotoxicity of silver nanoparticles in human embryonic stem cell-derived fibroblasts and an L-929 cell line. *Journal of Nanomaterials* **2012**, 2012, 9.

36. AshaRani, P.; Hande, M. P.; Valiyaveettil, S., Anti-proliferative activity of silver nanoparticles. *BMC Cell Biology* **2009**, 10, 65.

37. Ramirez-Lee, M. A.; Rosas-Hernandez, H.; Salazar-Garcia, S.; Gutierrez-Hernandez, J. M.; Espinosa-Tanguma, R.; Gonzalez, F. J.; Ali, S. F.; Gonzalez, C., Silver nanoparticles induce anti-proliferative effects on airway smooth muscle cells. Role of nitric oxide and muscarinic receptor signaling pathway. *Toxicol Lett* **2014**, 224, 246-56.

38. Cao, Y.; Roursgaard, M.; Kermanizadeh, A.; Loft, S.; Moller, P., Synergistic effects of zinc oxide nanoparticles and Fatty acids on toxicity to caco-2 cells. *Int J Toxicol* **2015**, 34, 67-76.

39. Baek, M.; Kim, M. K.; Cho, H. J.; Lee, J. A.; Yu, J.; Chung, H. E.; Choi, S. J., Factors influencing the cytotoxicity of zinc oxide nanoparticles: particle size and surface charge. *Journal of Physics: Conference Series* **2011**, 304, 7.

40. Bohmert, L.; Girod, M.; Hansen, U.; Maul, R.; Knappe, P.; Niemann, B.; Weidner, S. M.; Thunemann, A. F.; Lampen, A., Analytically monitored digestion of silver nanoparticles and their toxicity on human intestinal cells. *Nanotoxicology* **2014**, 8, 631-42.

41. NATO HANDBOOK ON THE MEDICAL ASPECTS OF NBC DEFENSIVE OPERATIONS AMedP-6(B). http://fas.org/nuke/guide/usa/doctrine/dod/fm8-9/toc.htm

42. Jaklevic, B.; Uyetake, L.; Lemstra, W.; Chang, J.; Leary, W.; Edwards, A.; Vidwans, S.; Sibon, O.; Tin Su, T., Contribution of Growth and Cell Cycle Checkpoints to Radiation Survival in Drosophila. *Genetics* **2006**, 174, 1963-72.

43. Yang, X.; Gondikas, A. P.; Marinakos, S. M.; Auffan, M.; Liu, J.; Hsu-Kim, H.; Meyer, J. N., Mechanism of silver nanoparticle toxicity is dependent on dissolved silver and surface coating in Caenorhabditis elegans. *Environ Sci Technol* **2012**, 46, 1119-27.

44. Kittler, S.; Greulich, C.; Diendorf, J.; Köller, M.; Epple, M., Toxicity of Silver Nanoparticles Increases during Storage Because of Slow Dissolution under Release of Silver Ions. *Chemistry of Materials* **2010**, 22, 4548-4554.

45. Cortese-Krott, M. M.; Munchow, M.; Pirev, E.; Hessner, F.; Bozkurt, A.; Uciechowski, P.; Pallua, N.; Kroncke, K. D.; Suschek, C. V., Silver ions induce oxidative stress and intracellular zinc release in human skin fibroblasts. *Free Radic Biol Med* **2009**, 47, 1570-7.

46. Walczak, A. P.; Fokkink, R.; Peters, R.; Tromp, P.; Herrera Rivera, Z. E.; Rietjens, I. M.; Hendriksen, P. J.; Bouwmeester, H., Behaviour of silver nanoparticles and silver ions in an in vitro human gastrointestinal digestion model. *Nanotoxicology* **2013**, 7, 1198-210.

47. Loeschner, K.; Hadrup, N.; Qvortrup, K.; Larsen, A.; Gao, X.; Vogel, U.; Mortensen, A.; Lam, H. R.; Larsen, E. H., Distribution of silver in rats following 28 days of repeated oral exposure to silver nanoparticles or silver acetate. *Part Fibre Toxicol* **2011**, 8, 18.

48. Saptarshi, S. R.; Duschl, A.; Lopata, A. L., Interaction of nanoparticles with proteins: relation to bio-reactivity of the nanoparticle. *J Nanobiotechnology* **2013**, 11, 26.

49. Shahare, B.; Yashpal, M., Toxic effects of repeated oral exposure of silver nanoparticles on small intestine mucosa of mice. *Toxicol Mech Methods* **2013**, 23, 161-7.

50. Kim, Y. S.; Song, M. Y.; Park, J. D.; Song, K. S.; Ryu, H. R.; Chung, Y. H.; Chang, H. K.; Lee, J. H.; Oh, K. H.; Kelman, B. J.; Hwang, I. K.; Yu, I. J., Subchronic oral toxicity of silver nanoparticles. *Part Fibre Toxicol* **2010**, 7, 20.

A)

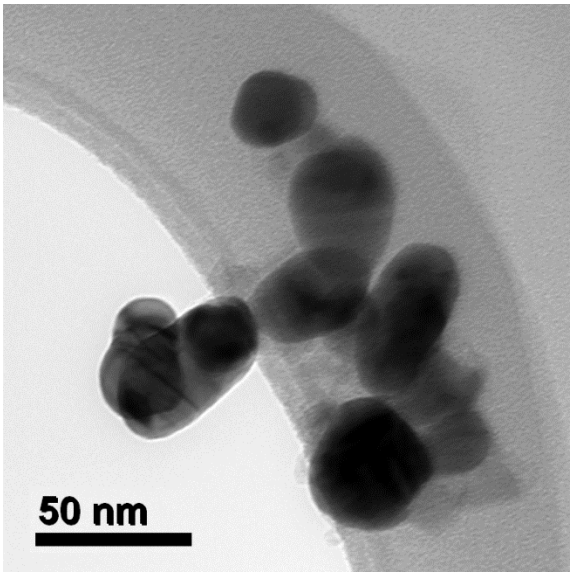
50 nm

B)

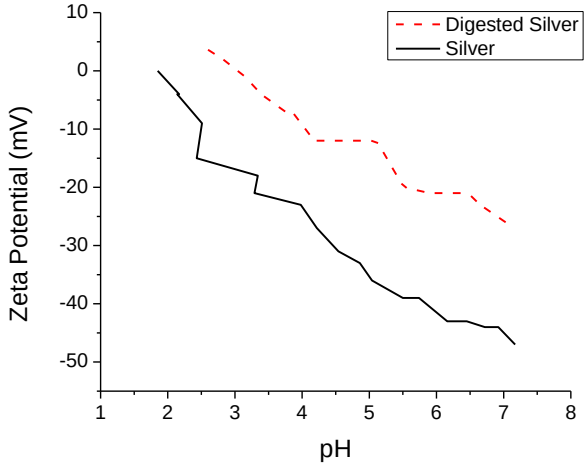
Digested Silver
Silver
Zeta Potential (mV)
10
0
-10
-20
-30
-40
-50
1
2
3
4
5
6
7
8
pH

C)

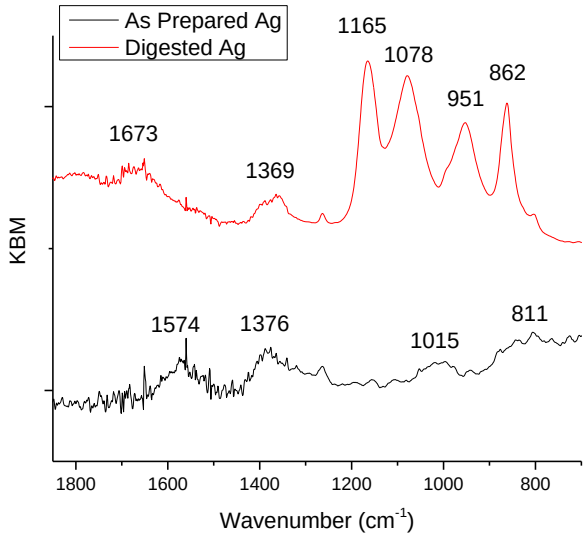
As Prepared Ag
Digested Ag
1165
1078
862
951
1673
1369
KBM
1574
1376
1015
811
1800
1600
1400
1200
1000
800
Wavenumber (cm-1)

D)

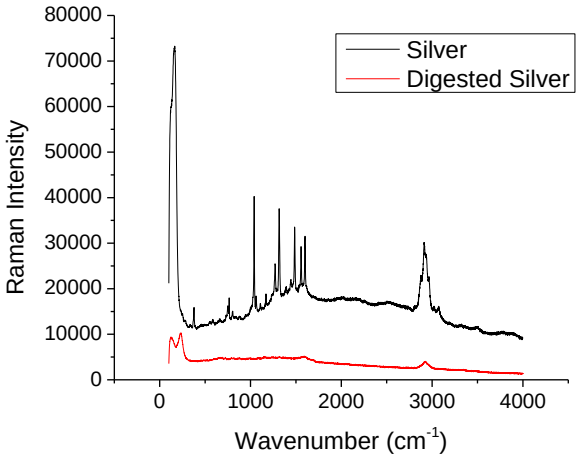
80000
70000
60000
50000
40000
30000
20000
10000
0
Raman Intensity
Silver
Digested Silver
0
1000
2000
3000
4000
Wavenumber (cm-1)

E)

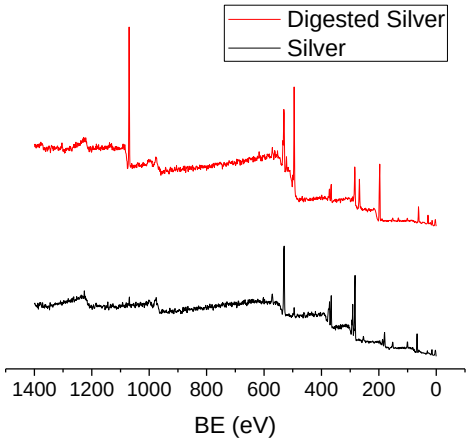

Figure 1: Characterization of pristine and digested Ag. A) TEM of pristine silver. Average diameter of Ag particles is 23 ± 8 nm. B) Zeta potential of pristine and digested Ag titrated from neutral to acidic pH. C) IR spectra of pristine and digested Ag. D) Raman spectra of pristine and digested Ag. E) XPS spectra of pristine and digested Ag (BE = binding energy).

A)

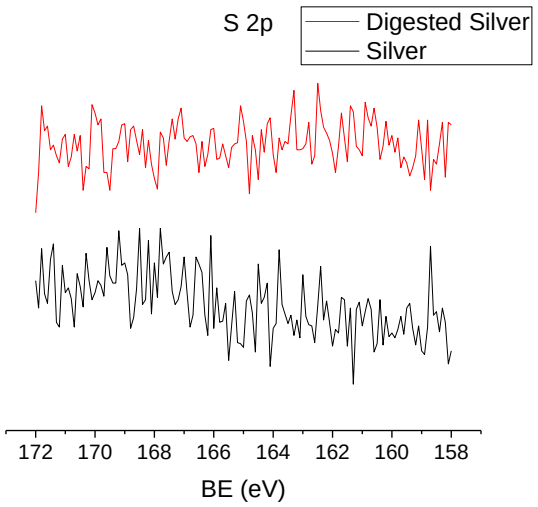
S 2p
Digested Silver
Silver
172
170
168
166
164
162
160
158
BE (eV)

B)

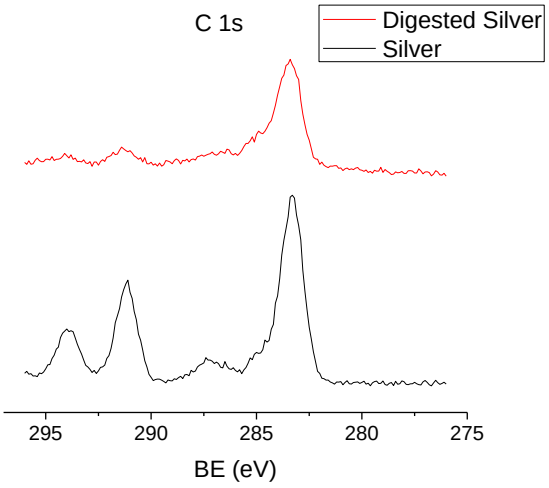
C 1s
Digested Silver
Silver
295
290
285
280
275
BE (eV)

C)

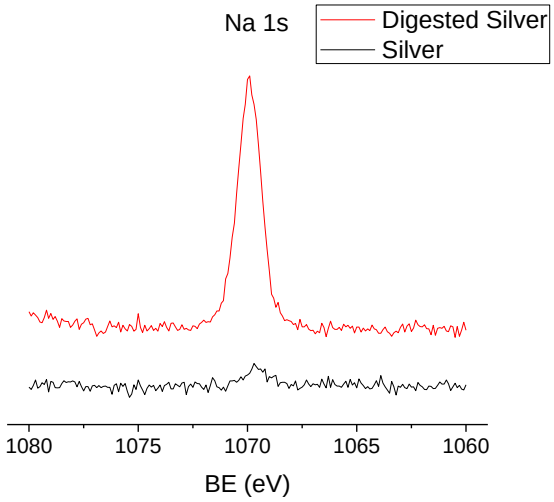
Na 1s
Digested Silver
Silver
1080
1075
1070
1065
1060
BE (eV)

D)

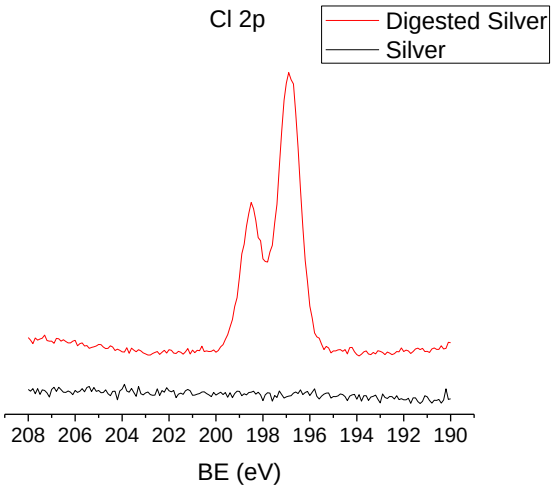
Cl 2p
Digested Silver
Silver
208 206 204 202 200 198 196 194 192 190
BE (eV)

E)

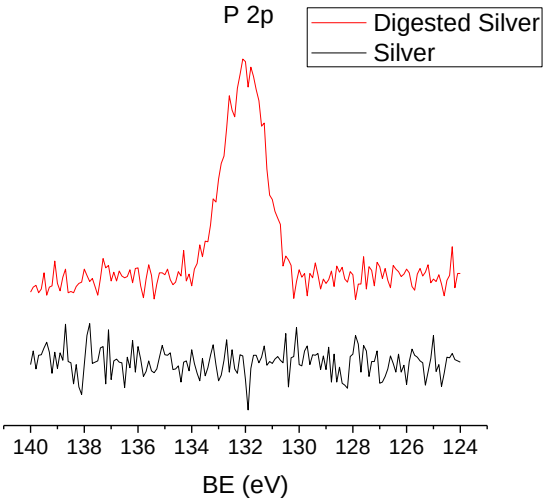
P 2p
Digested Silver
Silver
140 138 136 134 132 130 128 126 124
BE (eV)

F)

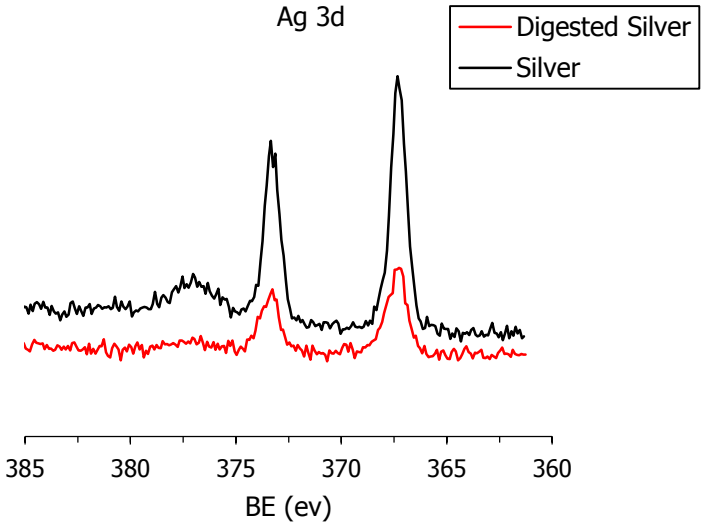
Ag 3d
Digested Silver
Silver
385
380
375
370
365
360
BE (ev)

G)

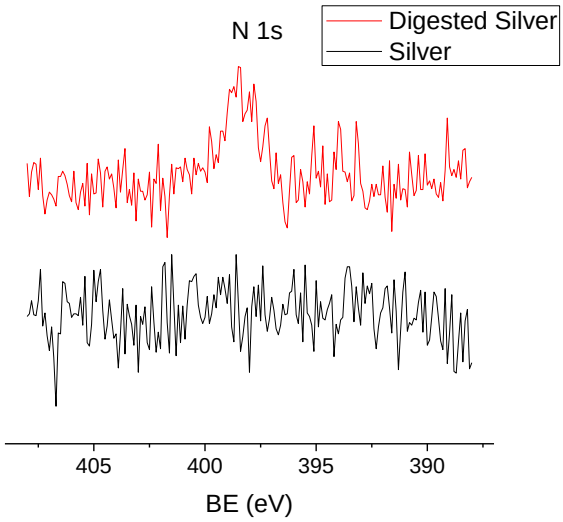
N 1s
Digested Silver
Silver
405
400
395
390
BE (eV)

H)

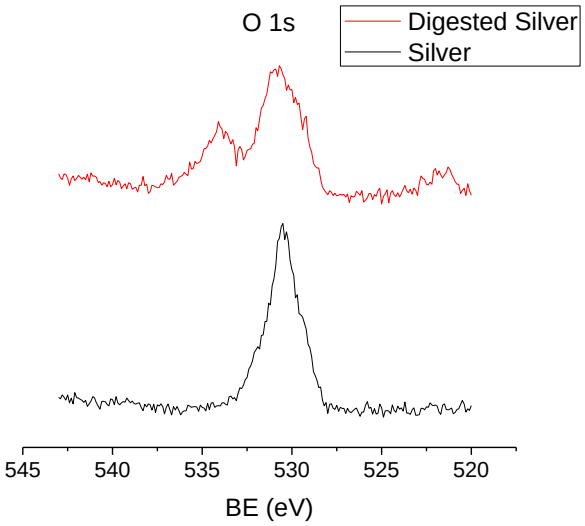

Figure 2: XPS spectra for both pristine and digested Ag NP corresponding to individual elements. XPS spectra for A) sulfur, B) carbon, C) sodium, D) chlorine, E) phosphorus, F) silver, G) nitrogen, and H) oxygen.

A)

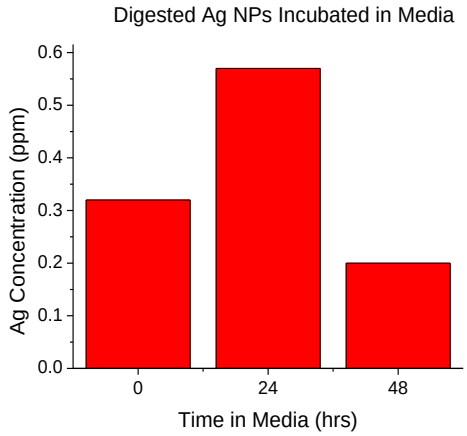

B)

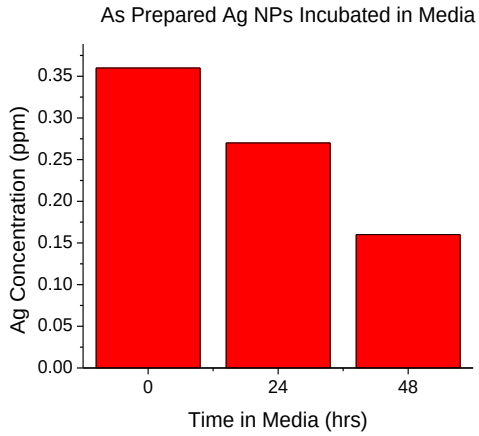

Figure 3: Stability of A) digested Ag and B) pristine Ag nanoparticles. Particles were incubated in cell culture media for up to 48 hours. Silver ions in solution were detected by atomic absorption spectroscopy at 0, 24, and 48 hours.

A)

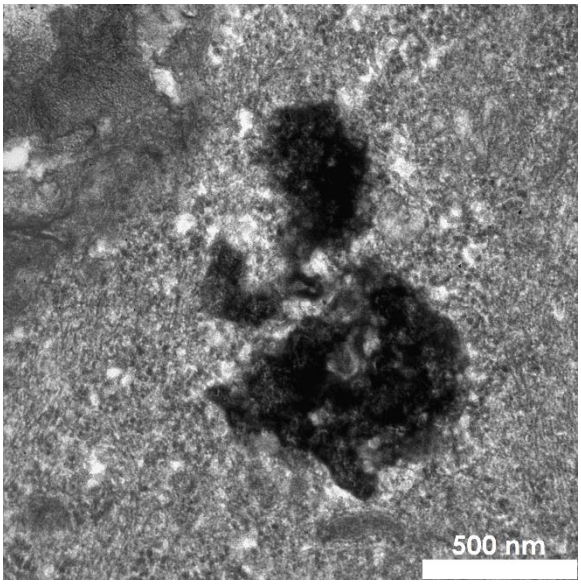

B)

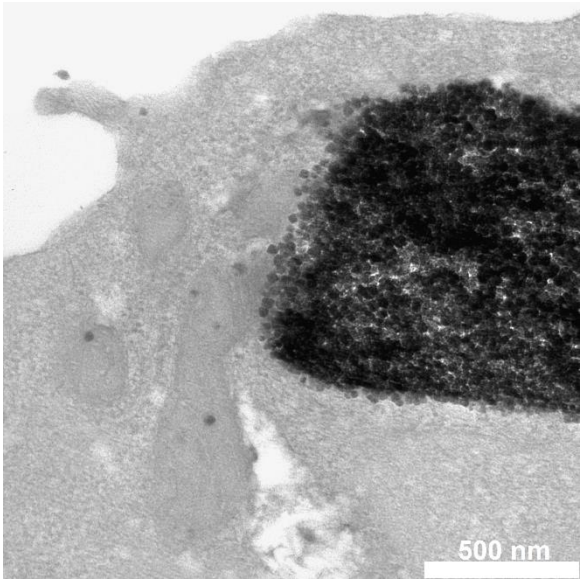

Figure 4: Internalization of Ag NP by intestinal epithelial cells *in vitro*. Cells were treated with A) pristine and B) digested Ag NP for 24 hours (10 μg/cm^2), then suspended, pelleted, and fixed for transmission electron microscopy.

A)

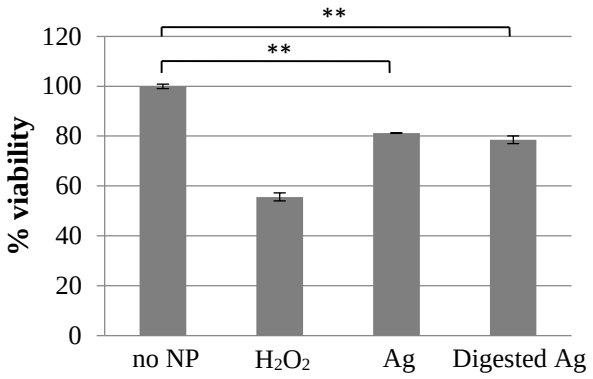
**
**
120
100
80
60
40
20
0
% viability
no NP
H2O2
Ag
Digested Ag

B)

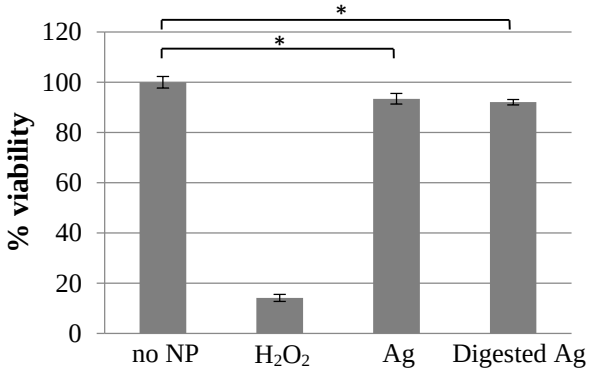
*
*
120
100
80
60
40
20
0
% viability
no NP
H2O2
Ag
Digested Ag

C)

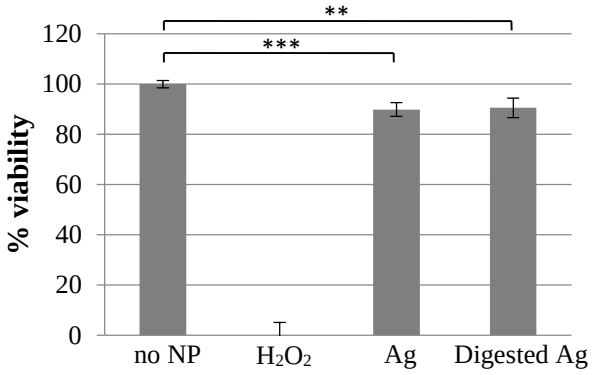
**
***
120
100
80
60
40
20
0
% viability
no NP
H2O2
Ag
Digested Ag

D)

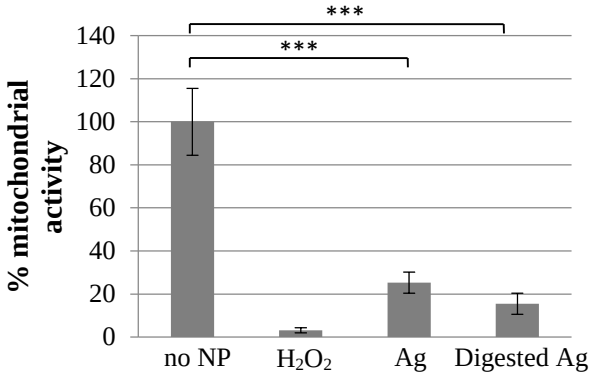
***
***
140
120
100
80
60
40
20
0
% mitochondrial activity
no NP
H2O2
Ag
Digested Ag

Figure 5: Toxicity assays performed on proliferating cells. Cells were plated at low density and allowed to adhere overnight. The following day cells were treated with 0.25 μg/cm^2 Ag and 0.5 μg/cm^2 digested Ag along with 20 mM H_2O_2 or 1% Triton X-100 as a positive control. A) Sytox Red staining and flow cytometric analysis of necrotic cells. B) Annexin V staining and flow cytometric analysis of apoptotic cells. Flow cytometric data were normalized such that the untreated cells were 100% viability and data are shown as the average of three replicates ± 1 standard deviation. C) LDH assay measuring cell membrane damage. D) MTT assay measuring mitochondrial activity of cells. LDH and MTT assay data are shown as the average of four replicates ± 1 standard deviation. Significance was calculated using Student's *t*-test (* indicates $p<0.05$; ** indicates $p<0.005$; *** indicates $p<0.0005$). Data are representative of two replicate experiments with the Sytox Red and Annexin V assays and one replicate experiment with LDH and MTT assays.

A) Ag

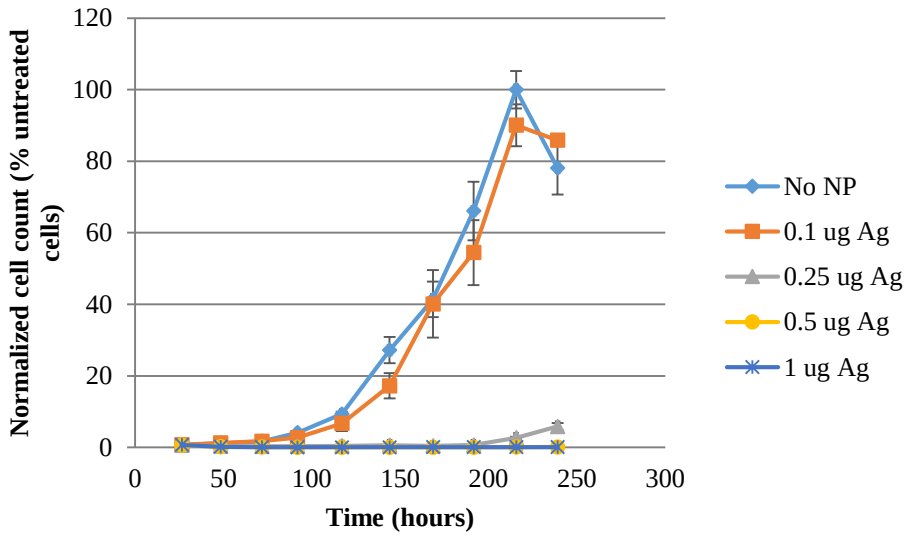

B) Digested Ag

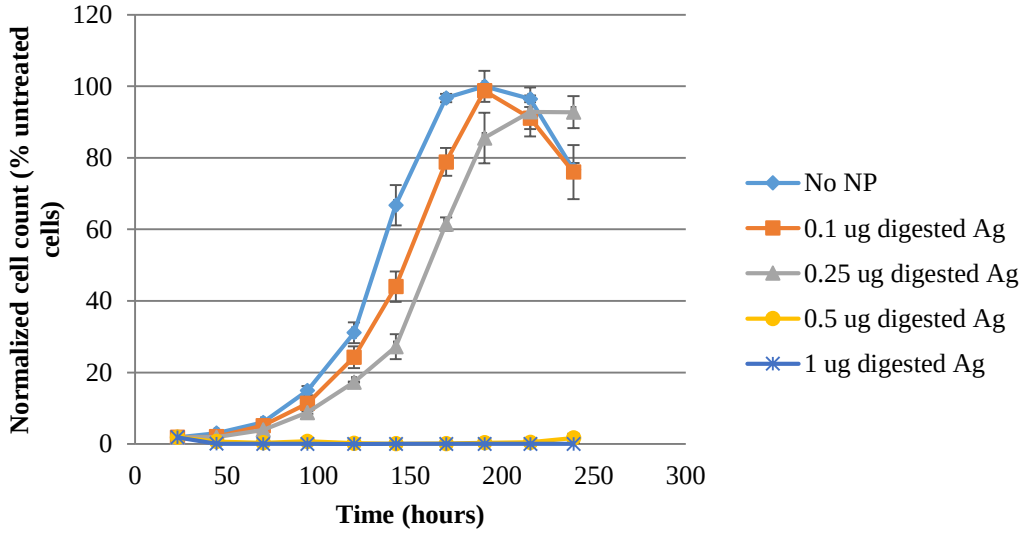

C) SiO_2

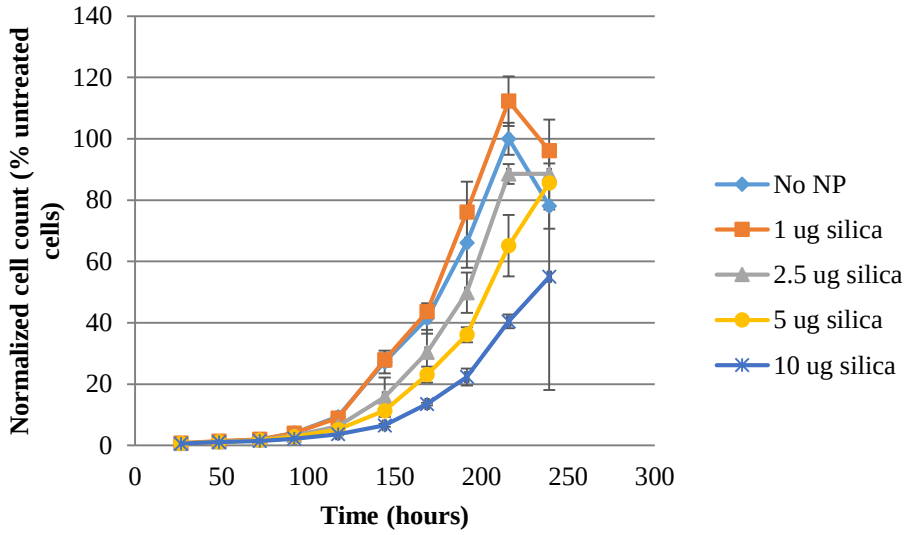
Normalized cell count (% untreated cells)
140
120
100
80
60
40
20
0
0
50
100
150
200
250
300
Time (hours)
No NP
1 ug silica
2.5 ug silica
5 ug silica
10 ug silica

D) TiO_2

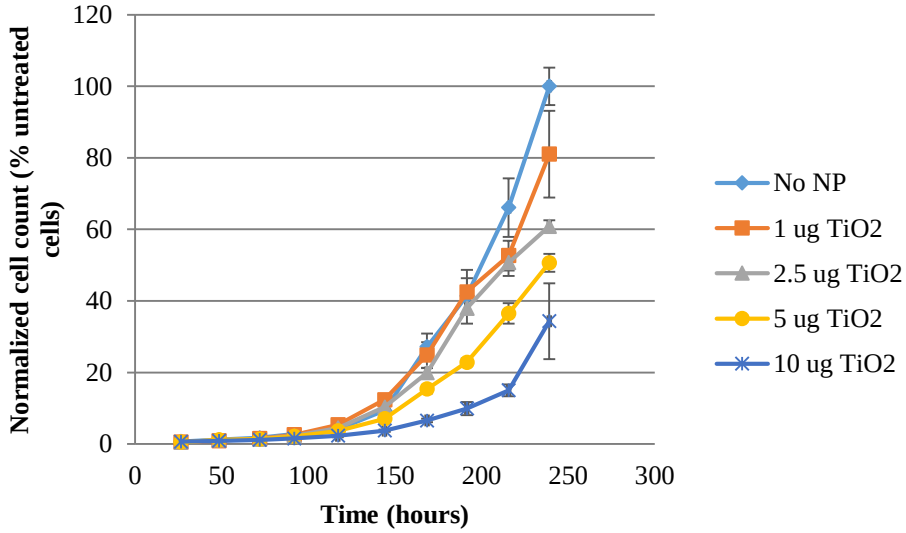
Normalized cell count (% untreated cells)
120
100
80
60
40
20
0
0
50
100
150
200
250
300
Time (hours)
No NP
1 ug TiO2
2.5 ug TiO2
5 ug TiO2
10 ug TiO2

E) ZnO

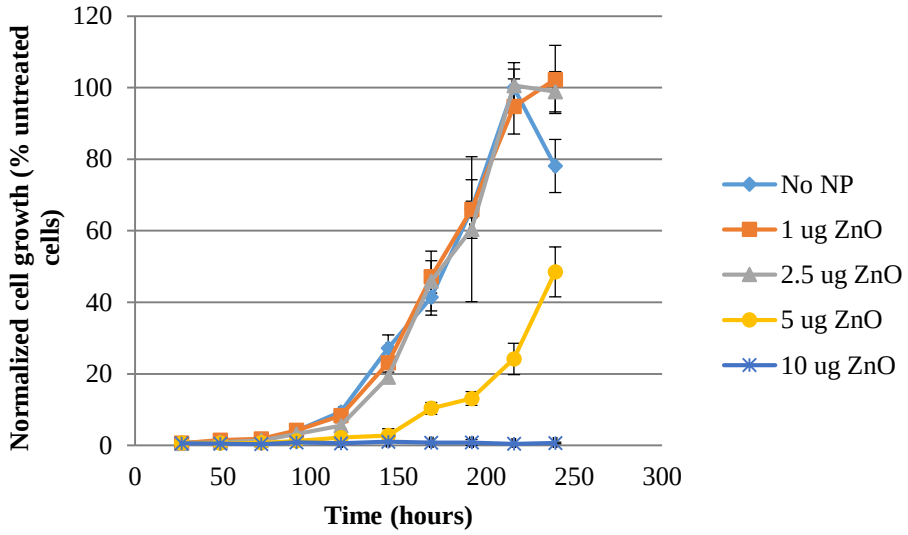

F) Zeolite

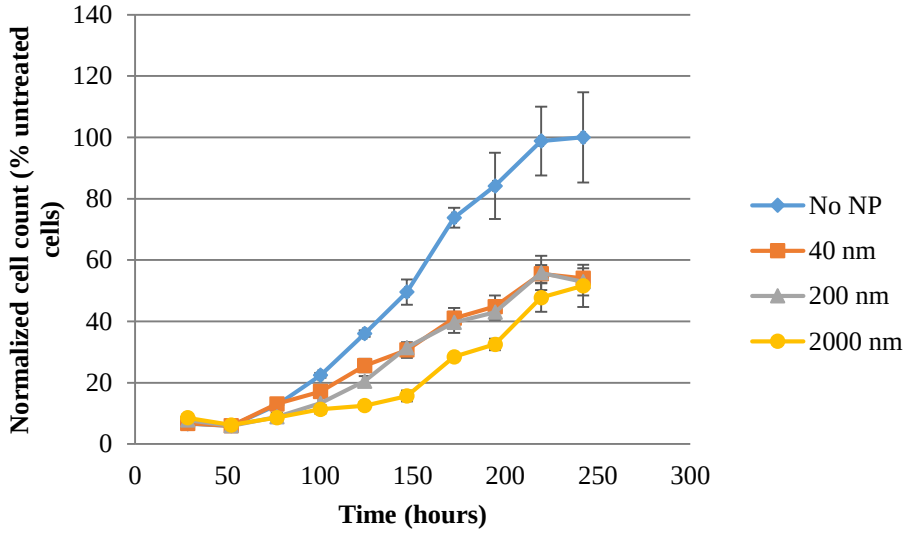

Figure 6: Inhibition of intestinal cell proliferation by food-relevant inorganic NP. Cells were plated at low density, allowed to adhere for 24 hours, then treated with various doses of A) pristine Ag, B) digested Ag, C) SiO_2, D) TiO_2, E) ZnO NP, or F) 10 µg/cm^2 of 40, 200, and 2000 nm zeolite particles. At 48-hour intervals NP-supplemented culture medium was replaced with fresh NP-supplemented medium. Samples of cells were counted at 24-hour intervals. Data points represent

mean normalized cell counts from 3 replicate wells ± 1 standard deviation (bars). Data were normalized to the maximum cell count for the untreated control cells as 100% cell growth. Data are representative of results of 3 replicate experiments with SiO_2, TiO_2, and ZnO, and pristine Ag, and 2 replicate experiments with digested Ag and zeolite.

A) Pristine Ag

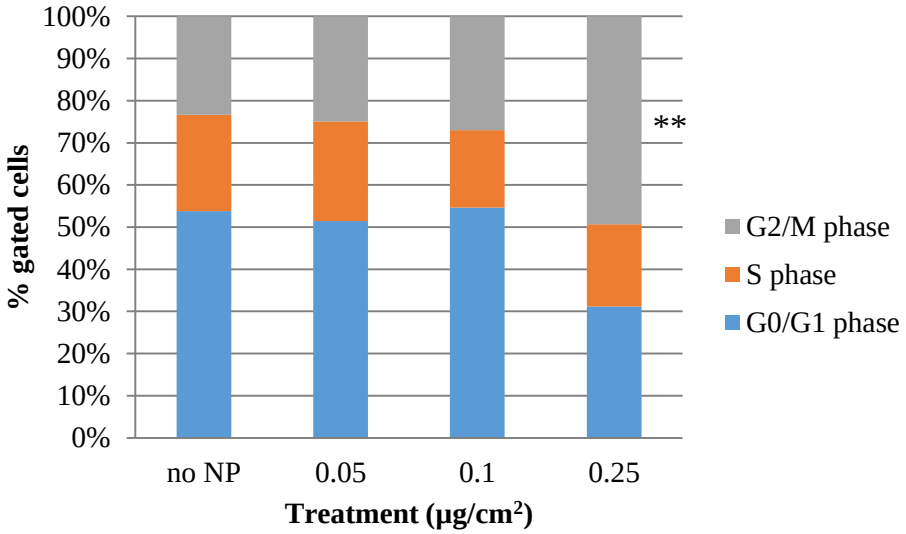

B) Digested Ag

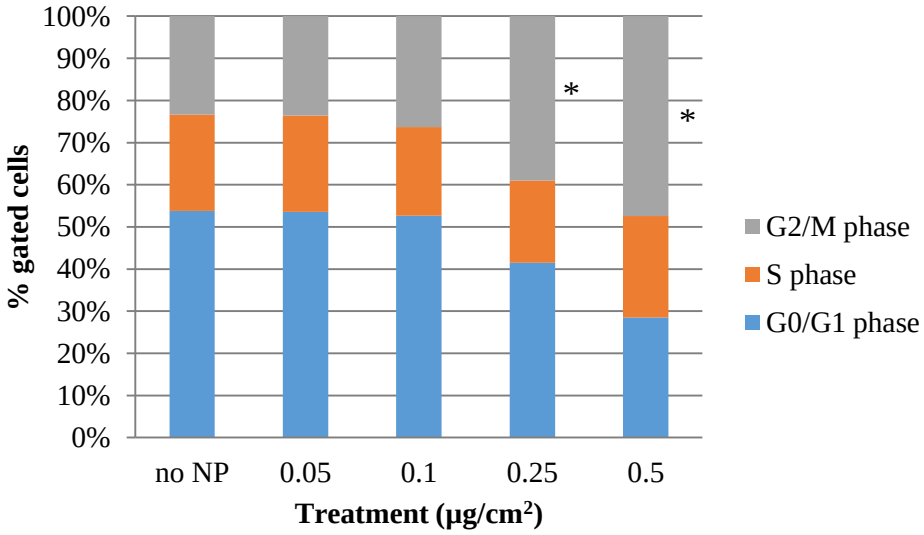

C) No NP

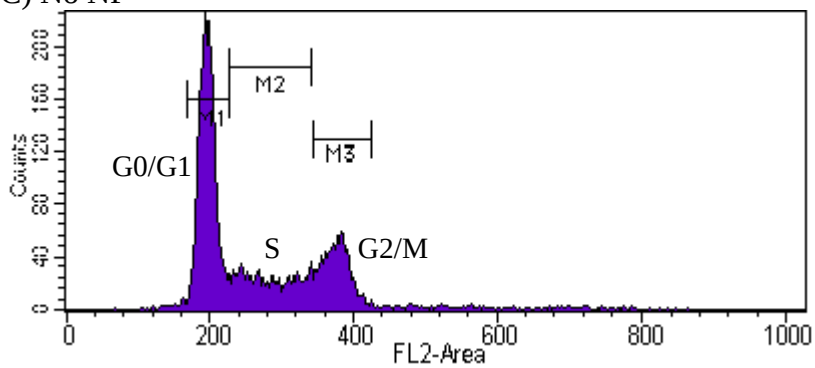

D) 0.25 µg/cm^2 pristine Ag

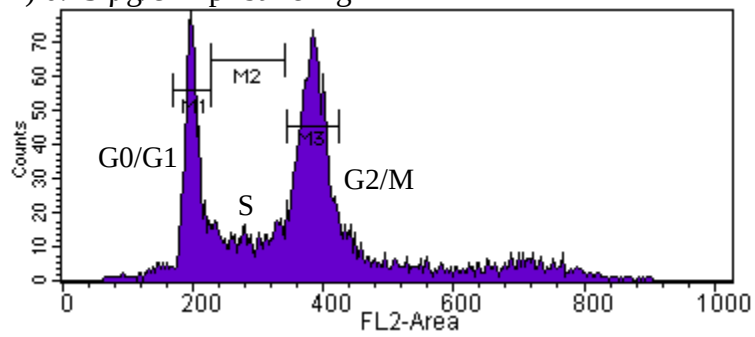

E) 0.5 µg/cm^2 digested Ag

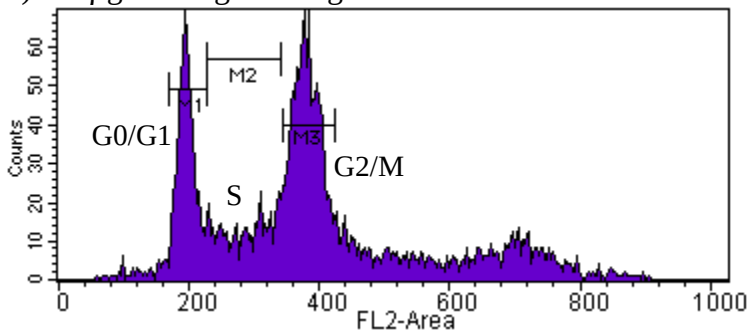

Figure 7: Cell cycle phase distribution (DNA content) of intestinal epithelial cells treated with pristine and digested Ag NP. Proliferating intestinal epithelial cells were treated with various doses of pristine and digested Ag NP continuously for 3 days. Cells were fixed, stained with propidium iodide, and DNA content was measured by fluorescence flow cytometry. Cell cycle phase was determined by DNA content: G0/G1 phase - 2n DNA, G2/M phase - 4n DNA, and S phase - 2n increasing to 4n. A) Cells were treated with increasing doses of pristine Ag NP or B) digested Ag NP and percentages of cells in each phase of the cell cycle were determined. Data shown are representative of 6 replicate experiments with pristine and digested Ag NP. Significance compared to G2/M phase untreated cells was measured by Student's *t*-test (* indicates $p<0.0005$; ** indicates $p<0.00005$). Representative flow cytometry histograms are shown for cells treated with C) no NP, D) 0.25 µg/cm^2 pristine Ag, and E) 0.5 µg/cm^2 digested Ag.

A)

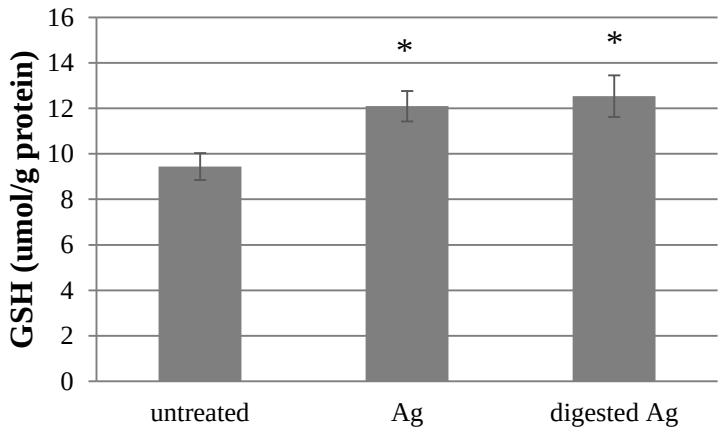
GSH (umol/g protein)
16
14
12
10
8
6
4
2
0
*
*
untreated
Ag
digested Ag

B)

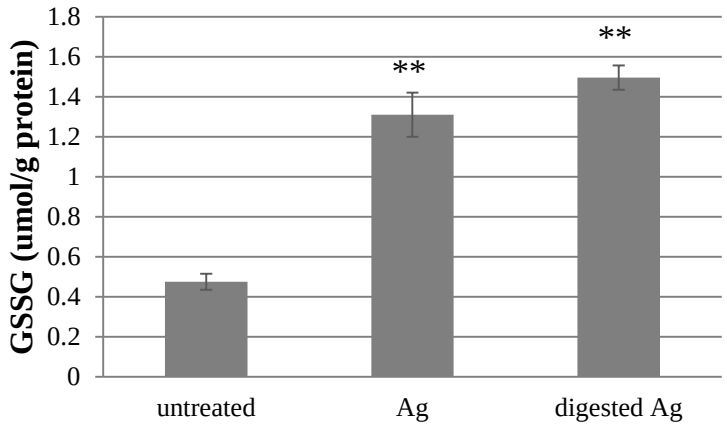
GSSG (umol/g protein)
1.8
1.6
1.4
1.2
1
0.8
0.6
0.4
0.2
0
**
**
untreated
Ag
digested Ag

C)

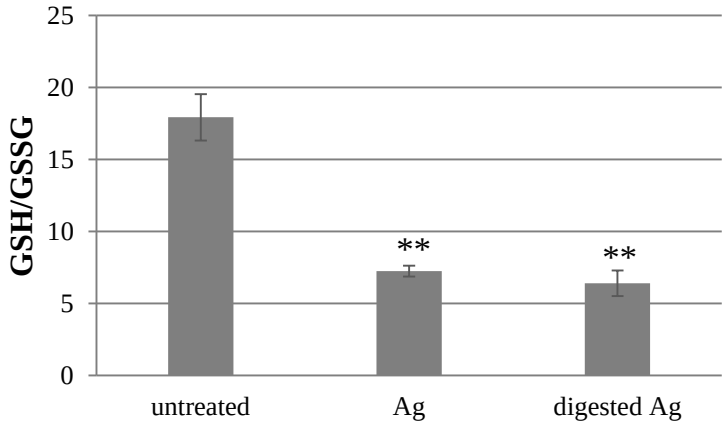
GSH/GSSG
25
20
15
10
5
0
**
**
untreated
Ag
digested Ag

D)

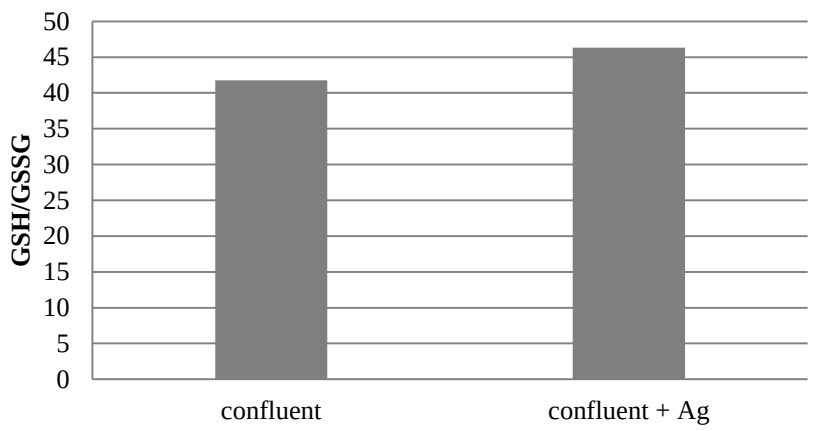

Figure 8: Levels of A) reduced glutathione (GSH), B) oxidized glutathione (GSSG), and C) GSH/GSSG ratio in cells treated with Ag NPs. Cells were plated at low density and allowed to adhere overnight before treating with Ag NPs for 24 hours. The cells were then harvested and GSH and GSSG levels were measured by luminescence. D) GSH/GSSG was measured in confluent cells treated with Ag NP. Graphs are representative of 5 experiments for pristine A, 3 experiments for digested Ag, and 3 experiments for the confluent cell data. Data represent mean concentrations for 3 replicate wells ± 1 standard deviation. Significance in comparison to untreated control was determined using Student's *t*-test (* represents p-value<0.01, ** represents p-value<0.0005).

A) No antioxidant

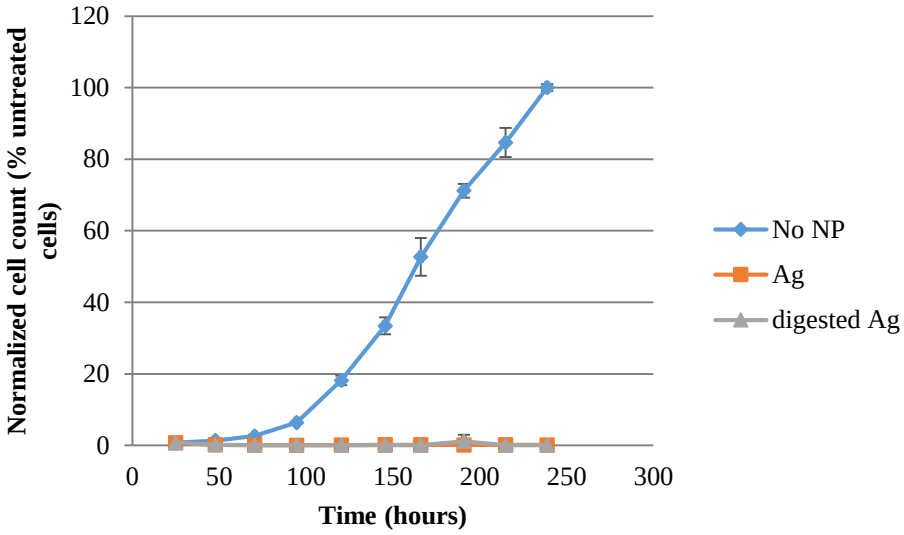

B) NAC

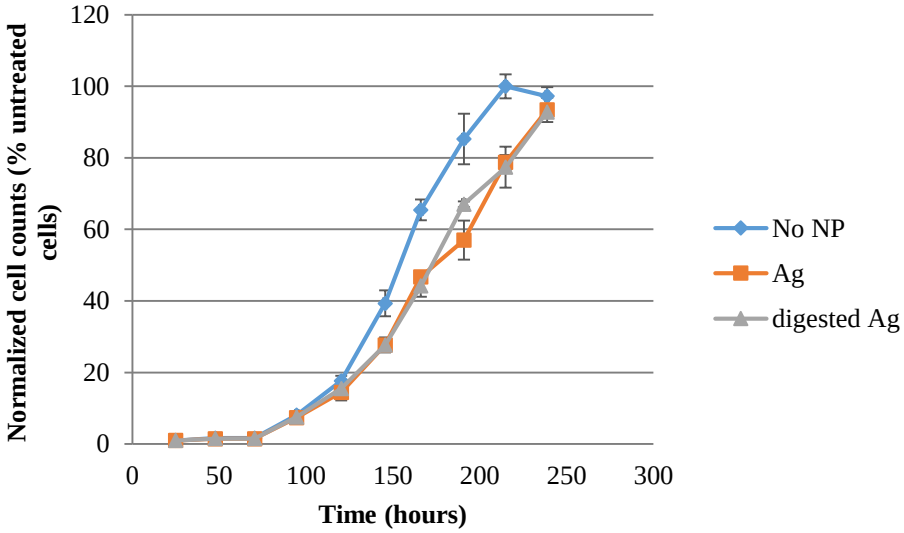

C) GSH/GSSG

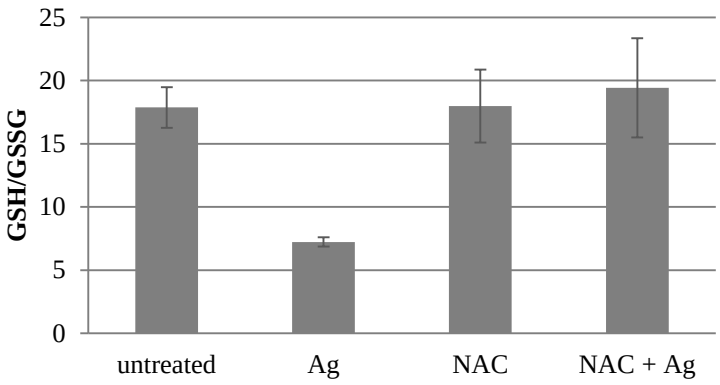

Figure 9: Impact of antioxidants and chelation upon Ag NP-mediated inhibition of cell proliferation and induction of oxidative stress. Intestinal epithelial cells were plated at low density, allowed to adhere for 24 hours, and then treated with A) no antioxidant or B) 10 mM NAC concurrent with the addition of 0.25 μg/cm^2 of pristine Ag NP or 0.5 μg/cm^2 digested Ag NP. Medium replenishment (including antioxidants and Ag NP) and cell counts were conducted as described above. Data represents normalized mean cell counts from 3 replicate wells ± 1 standard deviation (bars). Data were normalized to the maximum cell count for the untreated control cells as 100% cell growth. Data are representative of results of 2 replicate experiments. C) GSH/GSSG ratio measurements of cells plated at low density and treated with 0.25 μg/cm^2 Ag NP and 10 mM NAC for 24 hours. Data are representative of 3 replicate experiments. Data represent mean ratios for 3 replicate wells ± 1 standard deviation.

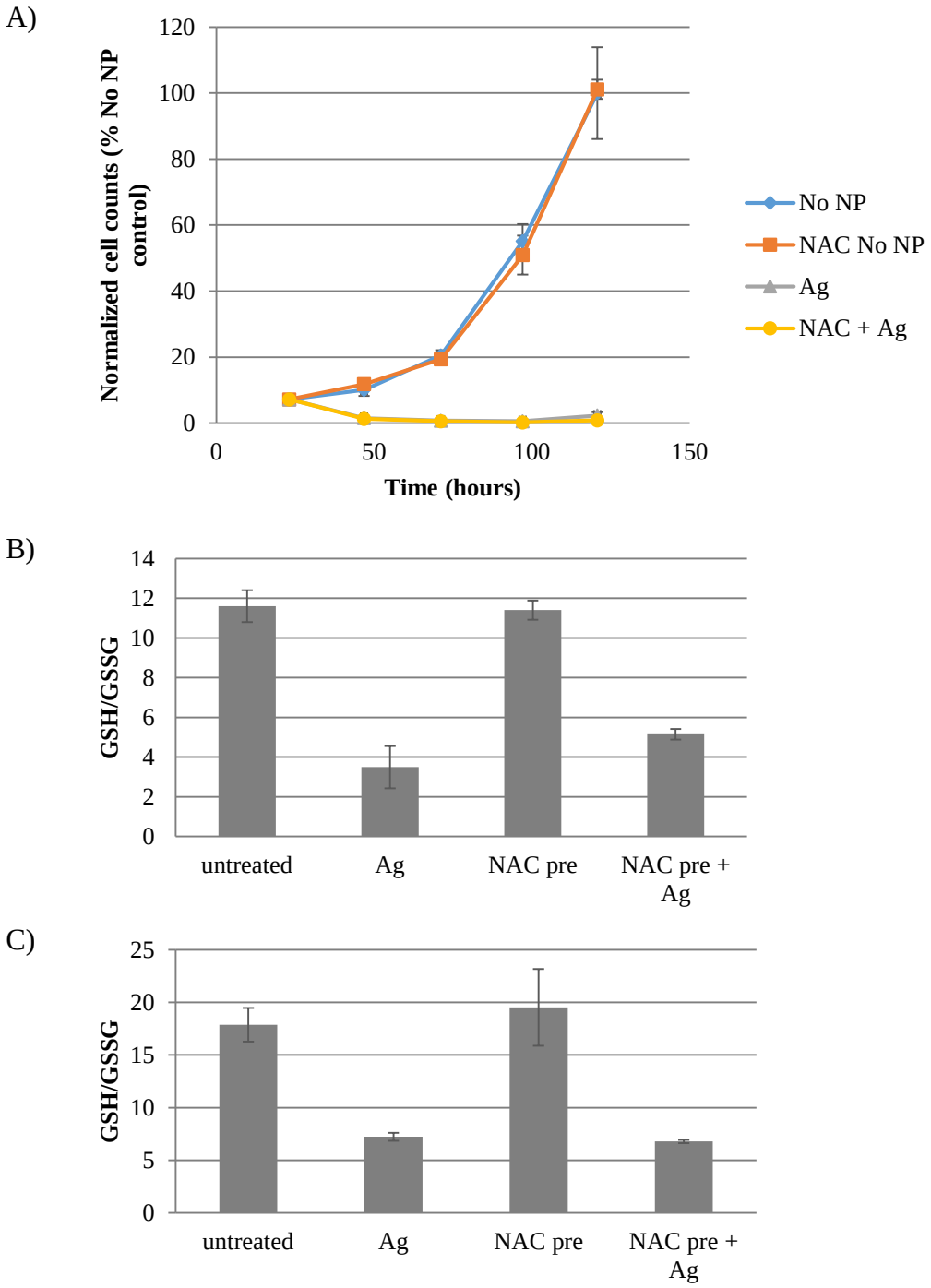

Figure 10: Cell growth and GSH/GSSG after pretreatment of cells with NAC prior to Ag NP exposure. Cells were plated at low density and treated with 0.25 µg/cm^2 Ag NP with or without 10 mM NAC treatment. A) Growth over five days of cells pre-treated with NAC for 1 hour before continuous Ag NP treatment. Data represent mean normalized cell counts of 3 replicate wells ± 1

standard deviation. Counts were normalized to the maximum growth observed for the untreated control cells as 100% growth. B) GSH/GSSG ratio measurements of cells treated with Ag NP and NAC together for 24 hours. C) GSH/GSSG ratio measurements of cells pre-treated with NAC for 1 hour before treatment of cells with Ag NP for 24 hours. Graphs are representative of 3 experiments for NAC at the same time as Ag, and 3 experiments for the NAC pre-treatment. Data represent mean concentrations for 3 replicate wells ± 1 standard deviation.

A) Sytox:

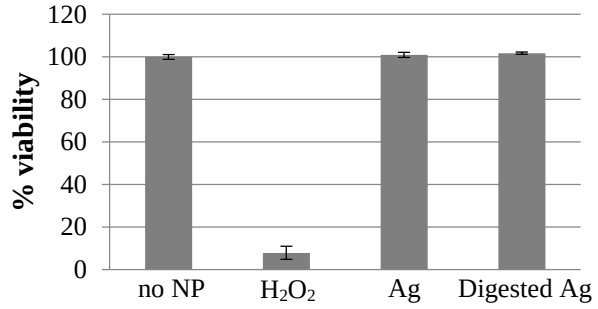

B) Annexin:

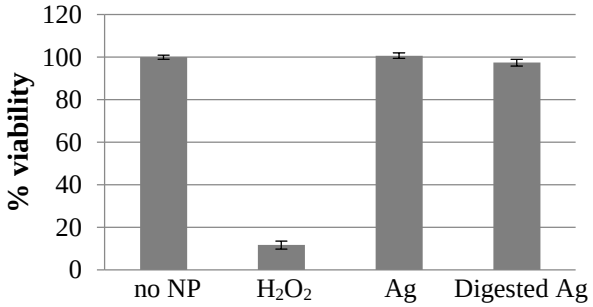

C) LDH:

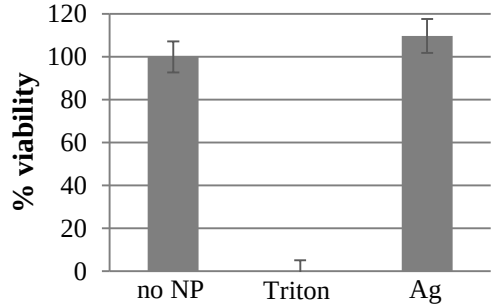

D) MTT:

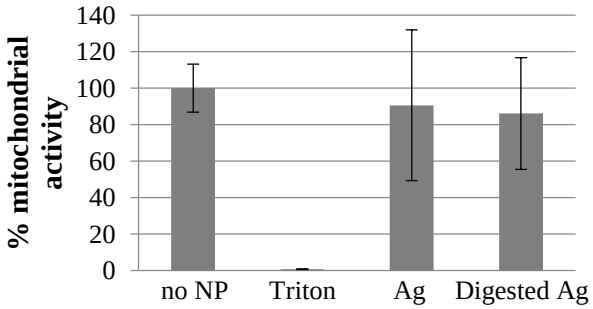

Figure 11: Acute toxicity in intestinal epithelial cells induced by Ag NP. Cells were treated with Ag NP for 24 hours (10 µg/cm^2) then analyzed by A) Sytox Red staining (necrosis), B) Annexin

V binding (apoptosis), C) LDH assay (cell membrane injury), and D) MTT assay (mitochondrial activity). Data represent means of three (Sytox Red, Annexin V) or four (LDH, MTT) replicate wells normalized to untreated control cells. The LDH assay was not used to determine digested Ag toxicity because we had previously found that the digestive enzymes interfere with the assay (McCracken et al. 2013). Error bars represent standard deviations. Data are compilations of two replicate experiments for Sytox Red, Annexin V, and LDH assays, and three replicate experiments for the MTT assay.

A)

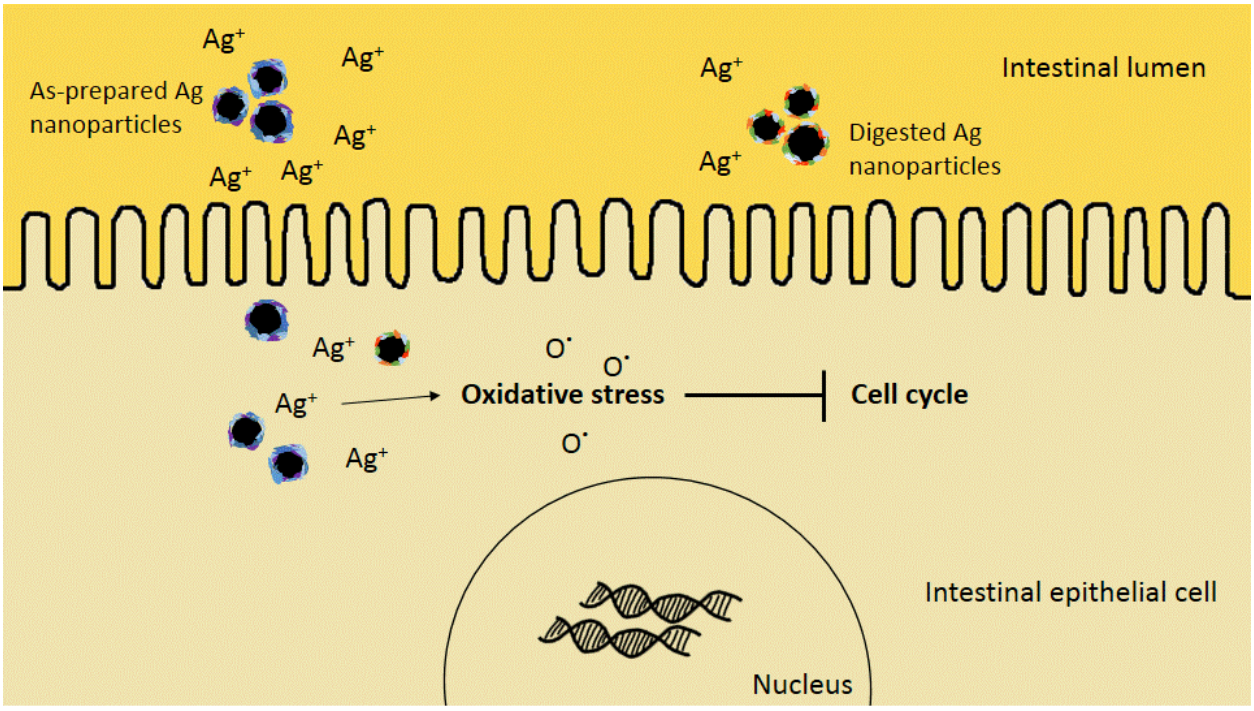
Ag+
Ag+
As-prepared Ag nanoparticles
Ag+
Ag+
Ag+
Ag+
Intestinal lumen
Digested Ag nanoparticles
Ag+
Ag+
Ag+
Ag+
O·
O·
Oxidative stress
Cell cycle
O·
Intestinal epithelial cell
Nucleus

B)

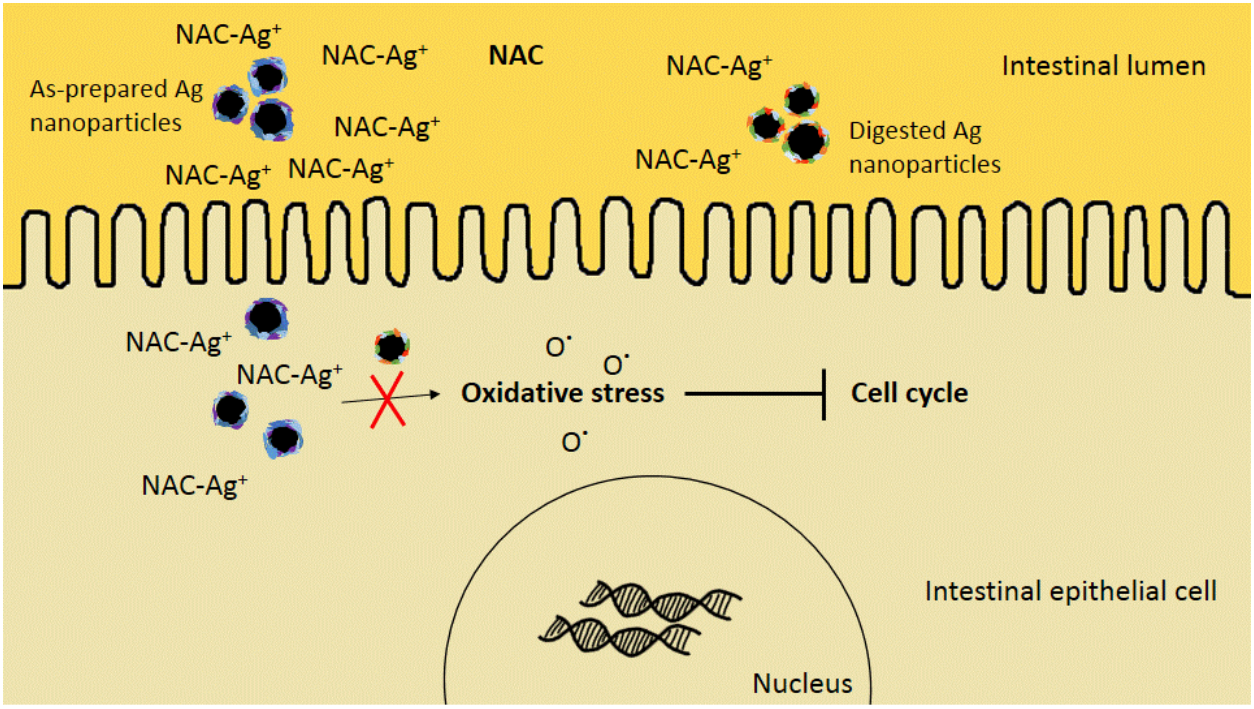
NAC-Ag+
NAC-Ag+
NAC
As-prepared Ag nanoparticles
NAC-Ag+
NAC-Ag+
NAC-Ag+
Intestinal lumen
NAC-Ag+
Digested Ag nanoparticles
NAC-Ag+
NAC-Ag+
NAC-Ag+
NAC-Ag+
O·
O·
Oxidative stress
Cell cycle
O·
NAC-Ag+
Intestinal epithelial cell
Nucleus

Figure 12: Mechanism of Ag NP toxicity. A) Ag NP are internalized by cells. Ag NP dissolution produces Ag ions available to interact with cells both inside and outside cells. Etc. Within cells, Ag NP induces oxidative stress which eventually leads to inhibition of cell proliferation. B) In the presence of NAC, complexes are formed with Ag^{+} which keeps the Ag from inducing oxidative stress.